

# Aurora B prevents chromosome arm separation defects by promoting telomere dispersion and disjunction

Céline Reyes,<sup>1,2\*</sup> Céline Serrurier,<sup>1,2\*</sup> Tiphaine Gauthier,<sup>1,2</sup> Yannick Gachet,<sup>1,2</sup> and Sylvie Tournier<sup>1,2</sup>

<sup>1</sup>Laboratoire de biologie cellulaire et moléculaire du contrôle de la prolifération, Université de Toulouse, F-31062 Toulouse, France

<sup>2</sup>Centre National de la Recherche Scientifique, LBCMCP-UMR5088, F-31062 Toulouse, France

**T**he segregation of centromeres and telomeres at mitosis is coordinated at multiple levels to prevent the formation of aneuploid cells, a phenotype frequently observed in cancer. Mitotic instability arises from chromosome segregation defects, giving rise to chromatin bridges at anaphase. Most of these defects are corrected before anaphase onset by a mechanism involving Aurora B kinase, a key regulator of mitosis in a wide range of organisms. Here, we describe a new role for Aurora B in telomere dispersion and disjunction during fission

yeast mitosis. Telomere dispersion initiates in metaphase, whereas disjunction takes place in anaphase. Dispersion is promoted by the dissociation of Swi6/HP1 and cohesin Rad21 from telomeres, whereas disjunction occurs at anaphase after the phosphorylation of condensin subunit Cnd2. Strikingly, we demonstrate that deletion of Ccq1, a telomeric shelterin component, rescued cell death after Aurora inhibition by promoting the loading of condensin on chromosome arms. Our findings reveal an essential role for telomeres in chromosome arm segregation.

## Introduction

The spatiotemporal control of mitotic events is essential to prevent the formation of aneuploid cells. During spindle formation, the kinetochores, protein structures that assemble at the centromeres of each pair of sister chromatids, attach to microtubules from opposite spindle poles. Subsequently, chromosomes align at the metaphase plate and once correctly bioriented, sister chromatids separate and move toward the poles because of the proteolytic cleavage of cohesin by the cysteine protease separase. Cohesin is a conserved and essential protein complex required for sister chromatid cohesion, which is composed of the two structural maintenance of chromosome (SMC) family proteins SMC1 and SMC3 and the two non-SMC subunits Rad21 (Uhlmann et al., 1999). Sister chromatid cohesion defines the correct back-to-back arrangement of sister kinetochores and prevents chromosome attachment defects such as merotelic attachment in which one kinetochore is attached to both poles (Gregan et al., 2007, 2011; Courtheoux et al., 2009; Sakuno et al., 2009). In fission yeast, the recruitment of cohesin at the

mating type locus, at outer repeat regions of centromeres, and at telomeric sites is dependent on the fission yeast heterochromatin protein 1 (HP1) homologue Swi6 through an interaction with Psc3 (Bernard et al., 2001; Nonaka et al., 2002) and the loading factor Mis4 (Fischer et al., 2009). HP1 proteins were originally identified as critical components in heterochromatin-mediated gene silencing (James et al., 1989; Clark and Elgin, 1992). These proteins possess an N-terminal chromodomain that specifically reads methylation of histone H3 at lysine 9 (H3K9me) and a chromoshadow domain that interacts with various effectors such as cohesin.

The Aurora B kinase is required for the fidelity and the coordination of mitotic processes. Aurora B is one of the chromosomal passenger complex (CPC) proteins, first identified in vertebrates as proteins that move from centromeres to the spindle midzone at the metaphase-to-anaphase transition (Carmena et al., 2012). The CPC regulates key mitotic events such as chromosome compaction, correction of chromosome-microtubule attachment errors, spindle assembly checkpoint control, central spindle formation, and the regulation of furrow ingression and

\*C. Reyes and C. Serrurier contributed equally to this paper.

Correspondence to Sylvie Tournier: sylvie.tournier-gachet@univ-tlse3.fr; or Yannick Gachet: yannick.gachet@univ-tlse3.fr

Abbreviations used in this paper: CPC, chromosomal passenger complex; HP1, heterochromatin protein 1; rDNA, ribosomal DNA; SMC, structural maintenance of chromosome; SPB, spindle pole body.

© 2015 Reyes et al. This article is distributed under the terms of an Attribution-Noncommercial-Share Alike-No Mirror Sites license for the first six months after the publication date (see <http://www.rupress.org/terms>). After six months it is available under a Creative Commons License [Attribution-Noncommercial-Share Alike 3.0 Unported license, as described at <http://creativecommons.org/licenses/by-nc-sa/3.0/>].

abscission (Sampath et al., 2004; Kotwaliwale et al., 2007; Mora-Bermúdez et al., 2007; Steigemann et al., 2009; Tada et al., 2011). The substrates of Aurora B in these different steps of mitosis are beginning to be elucidated (Koch et al., 2011; Carmena et al., 2012). Notably, the CPC regulates the binding of condensin, a multimeric protein complex essential for the maintenance of mitotic chromosome architecture (Giet and Glover, 2001; Morishita et al., 2001; Ono et al., 2004). In fission yeast, Aurora B-dependent phosphorylation of the kleisin Cnd2 promotes condensin recruitment to chromosomes (Nakazawa et al., 2011; Tada et al., 2011). Similarly, in human cells, phosphorylation of kleisin by Aurora B promotes efficient association of condensin I to mitotic chromosomes (Ono et al., 2004; Lipp et al., 2007; Tada et al., 2011).

In *Schizosaccharomyces pombe*, homologues of the CPC, Bir1/Survivin, Pic1/INCENP, and Ark1/Aurora B are major regulators of mitosis (Morishita et al., 2001; Petersen et al., 2001; Leverson et al., 2002). Inhibition of Aurora B using a Shokat mutant leads to chromosome segregation defects (Koch et al., 2011), such as merotelic or syntelic attachment (Gay et al., 2012), and condensin is thought to be the main target of Aurora B at the kinetochore (Nakazawa et al., 2011; Tada et al., 2011). Aurora B colocalizes with kinetochores during metaphase and redistributes to the spindle midzone at anaphase onset in several organisms including fission yeast (Petersen et al., 2001). In addition, it has been shown to colocalize with telomeres in mitosis using either microscopy or chromatin immunoprecipitation approaches (Vanoosthuyse et al., 2007; Yamagishi et al., 2010). Although the kinetochore function of Aurora B in chromosome attachment and segregation has been extensively studied in several organisms (Tanaka et al., 2002; Ditchfield et al., 2003; Pinsky et al., 2006; Hauf et al., 2007), the role of Aurora B at telomeres is presently unknown.

The organization of telomeres into foci within the nuclear space is essential for the control of gene activation, gene silencing, and DNA repair (Palladino et al., 1993; Gotta and Gasser, 1996; Maillet et al., 1996; Hediger et al., 2002; Sexton et al., 2007; Misteli and Soutoglou, 2009). In fission yeast, the telomeres are located at the nuclear periphery in two to four clusters (Funabiki et al., 1993). This focal organization depends on heterochromatin (Ekwall et al., 1996; Alfredsson-Timmins et al., 2007) and is affected by mutations in the key RNAi factors Ago1, Dcr1, and Rdp1 (Hall et al., 2003). How the disjunction of telomere foci is controlled during chromosome segregation remains unknown.

In this study, we demonstrate that the fission yeast Aurora kinase Ark1 promotes telomere dispersion and disjunction in mitosis. Aurora controls telomere dispersion in metaphase by promoting the dissociation of Swi6/HP1 and cohesin Rad21 from telomeres. Subsequently, Aurora promotes telomere disjunction and chromosome arm separation by phosphorylating the condensin subunit Cnd2. Strikingly, deletion of the telomere-specific shelterin complex component Ccq1 is sufficient to bypass Aurora B-dependent defects in telomere dispersion and disjunction. Hence, this telomere-specific mechanism can prevent the formation of anaphase chromatin bridges in dividing cells.

## Results

### Telomere clusters dissociate in two steps during mitosis

To investigate whether telomere disjunction is subject to cell cycle regulation, we performed live imaging of cells endogenously expressing a nuclear envelope marker, Amo1-rfp (Pardo and Nurse, 2005), a spindle pole body (SPB) marker, Cdc11-cfp (Tournier et al., 2004), and a telomere marker protein, Taz1-gfp—a homologue of mammalian TRF1/TRF2 that binds exclusively to telomere repeats (Cooper et al., 1997; Vassetzky et al., 1999; Chikashige and Hiraoka, 2001; Fig. 1 A). Fission yeast has three chromosomes. During interphase, telomeres organized in one to three clusters in 96% of cells ( $n = 456$ ; Fig. 1 A), but as cells progressed through mitosis, the number of Taz1 spots gradually increased to a maximum of 12 as a function of spindle length (Fig. 1 B). In early mitosis, the telomere clusters were still intact (Fig. 1 B, red diamonds), suggesting that cluster dispersion may occur at the metaphase-to-anaphase transition. To address this point, we followed individual *taz1-gfp cdc11-cfp*-expressing cells through mitosis. In early mitosis, also called phase 1 in fission yeast, a short spindle (up to 2.0  $\mu\text{m}$ ) is formed, as judged by SPB separation. In phase 2, this spindle length is maintained until sister chromatid separation (anaphase A). Phase 3 consists entirely of anaphase B, during which the spindle elongates along the long axis of the cell. We find that telomere cluster dispersion is initiated (from one to two foci) in phases 1 and 2, before anaphase A, and clusters fully dissociate during anaphase B (phase 3) when the chromosome arms are separated (telomere disjunction, from 6 to 12 foci; Fig. 1, C and D). An example of mitotic telomere dispersion and disjunction is shown in a single cell analysis (Fig. 1 C) together with a quantification of Taz1 foci during mitotic progression (Fig. 1 D).

During telophase, the spindle disassembles, the two SPBs move back to the center of the cell, and the telomeres form new clusters (Fig. S1 A). Quantification of Taz1 foci confirmed that the reestablishment of Taz1 clusters occurs after spindle disassembly and the onset of cytokinesis, as judged by the movement of the SPBs toward the cell center (Fig. S1, B and C). Together, these experiments suggest that telomere clustering is regulated through the cell cycle and that cluster separation occurs in two steps, namely, telomere dispersion before anaphase onset followed by telomere disjunction during anaphase B.

### Aurora B kinase controls sister chromatid telomere dispersion and disjunction

We performed live imaging of cells simultaneously expressing markers for the SPBs (Cdc11-cfp), telomeres (Taz1-rfp), and Aurora B (Ark1-gfp). In addition to its well-known localization at the kinetochore and the spindle midzone (Adams et al., 2001; Giet and Glover, 2001), Aurora B also colocalized, transiently, to the telomeres in metaphase (Fig. 2 A, 0–3 min, arrows). Localization to the telomeres was not observed after anaphase onset (Fig. 2 A, 4 and 5 min).

To test the function of Aurora B in telomere disjunction, we used ATP analogue sensitive alleles of Aurora B (Shokat mutant *ark1-as3*; Hauf et al., 2007). *Cdc25-22 ark1-as3* cells

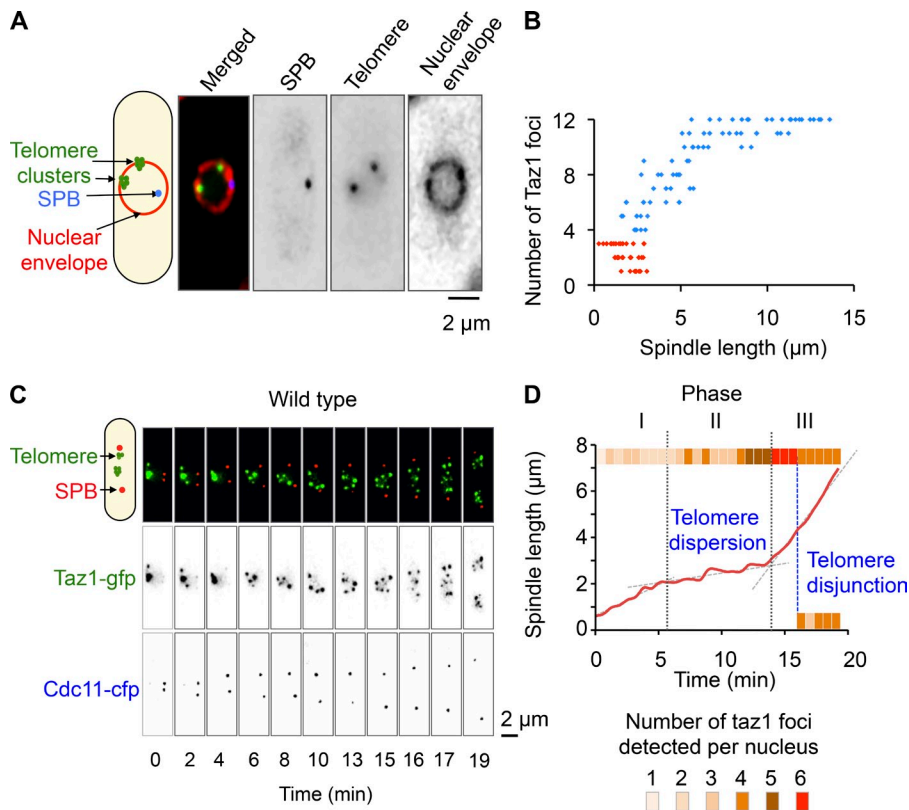


**Figure 1. Telomere cluster dispersion and disjunction occurs gradually in mitosis from metaphase up to anaphase B.** (A) Image of a wild-type cell expressing Taz1-gfp (telomeres, green), Cdc11-cfp (SPB, blue), and Amo1-rfp (nuclear envelope, red) during interphase. (B) Analysis of the number of Taz1 foci according to spindle length before telomere re-clustering. The data shown are from a single representative experiment out of three repeats. For the experiment shown,  $n = 119$ . The red dots represent clusters of telomeres (defined as a maximum of one to three foci), whereas blue dots represent the initiation of telomere dispersion and disjunction (more than three foci). (C) Movie of a cell expressing Taz1-gfp (green) and Cdc11-cfp (blue) through mitotic progression. (D) Analysis of the cell shown in C illustrating the precise timing of telomere dispersion and disjunction according to spindle length. The number of Taz1 foci is shown with a color code for each nucleus. Multiple cells were analyzed and behave in a similar manner. Note that during phase 1 (prophase) and phase 2 (metaphase) a single nucleus is observed, whereas in phase 3 (anaphase B) the number of Taz1 foci for each nucleus is shown.

expressing telomere (*taz1-gfp*, green; *pot1-rfp*, red), kinetochore (*ndc80-gfp*, green), centromere (*mis6-rfp*, red), and SPB markers (*cdc11-cfp*, blue) were synchronized in G2 (36°C) and released into mitosis (25°C) for 10 min (>80% of cells were in phase I; Fig. 2 B). Aurora B activity was specifically inhibited in early mitosis by adding the ATP analogue Napp1 (10  $\mu$ M; Fig. 2 B). Single cell analysis of telomere disjunction with respect to spindle size shows that Aurora inhibition significantly reduced the number of Taz1 foci, even after full spindle elongation (Fig. 2 C). In cells with fully elongated spindles, kinetochores were correctly segregated in  $48 \pm 0.7\%$  of the cells ( $n = 179$ ; as judged by the Mis6/Ndc80 kinetochore signals) but telomeres remained as clusters at the spindle midzone (Fig. 2 D). Interestingly, although Pot1 was lost from telomeres in control cells during mitosis, it remained strongly associated with telomeres when Aurora was inhibited.

In fission yeast, both arms of chromosome III interact directly with the nucleolus, the main bulk of the ribosomal DNA (rDNA) being located close to the telomeres (Uzawa and Yanagida, 1992). To investigate the position of telomere clusters relative to the nucleolus, we performed live imaging of cells simultaneously expressing the fission yeast fibrillarin (Fig. S2 A, Fib1-rfp, red; Beauregard et al., 2009), an SPB marker (Cdc11-cfp, blue), and a telomere protein marker (Taz1-gfp, green). In wild-type cells, telomeres localized in close proximity to the nucleolus and full telomere disjunction was always coordinated with nucleolar segregation (Fig. S2 A, left). Interestingly, Aurora B inhibition blocked both telomere disjunction and nucleolar segregation in  $86 \pm 2\%$  ( $n = 293$ ) of cells (Fig. S2 A, right). These experiments demonstrate that Aurora B

kinase activity controls telomere dispersion, sister chromatid telomere disjunction, and nucleolar segregation in anaphase.

### Telomere nondisjunction mechanically disturbs spindle elongation and leads to the formation of anaphase chromatin bridges

Aurora B inhibition causes several types of chromosome attachment defects in mitosis, e.g., merotelic attachments (Tanaka et al., 2002; Cimini et al., 2006; Knowlton et al., 2006), which antagonize the spindle elongation rate (Courtheoux et al., 2009). Because merotelic attachments are partly corrected during anaphase B by spindle elongation forces (Courtheoux et al., 2009), it seems unlikely that the lethality of Aurora-inhibited cells arises from this type of defect. We thus analyzed the impact of telomere nondisjunction on spindle elongation. We followed the changes in spindle elongation in single cells (*cdc25-22 ark1-as3* synchronised in G2) expressing markers for telomeres (Fig. 3 A, *taz1-gfp*, green), kinetochores (*ndc80-gfp*, green), centromeres (*mis6-rfp*, red), and SPBs (*cdc11-cfp*, blue). In control cells (Fig. 3, A and B, gray), the spindle elongation rate was  $0.87 \pm 0.09 \mu\text{m}/\text{min}$ . As expected, inhibition of Aurora B in metaphase led to the appearance of merotelic attachments in anaphase as judged by the appearance of stretched kinetochores (Fig. 3, A and B, red). Concomitantly, the spindle elongation rate was halved ( $0.39 \pm 0.12 \mu\text{m}/\text{min}$ ). In cells lacking merotelic attachments it was possible to observe the impact of the nondisjunction of chromosome arms on mitotic progression (Fig. 3, A and B, green). In such cells, DAPI staining revealed the presence of fine chromatin bridges with fully separated kinetochores

**Figure 2. Aurora B kinase colocalizes with telomeres in metaphase and controls sister chromatid telomere dispersion and disjunction.** (A) Movie of a cell expressing Taz1-rfp (telomeres, red), Ark1-gfp (Aurora, green), and Cdc11-cfp (SPB, blue) during mitotic progression. In metaphase (first four panels), Aurora transiently colocalizes to telomeres (arrows), whereas in anaphase (last two panels), it is absent from telomeres and present at the spindle midzone. (B) Schematic description of the procedure used to specifically inhibit Aurora kinase in early mitosis. (C) *cdc25-22 ark1-as3* (red,  $n = 98$ , and black,  $n = 62$ ) or *cdc25-22* (gray,  $n = 60$ ) cells were synchronized in G2 (36°C) and released in metaphase (25°C) before adding 10  $\mu$ M Napp1 (Aurora inhibition). Synchronized mitotic cells were filmed through mitosis in the presence (Aurora inhibition, red) or absence (No inhibition or control, gray and black) of 10  $\mu$ M Napp1 and the number of Taz1 dots was counted according to spindle length. The data shown are from a single representative experiment out of three repeats. (D) Example of the phenotypes seen in *cdc25-22 ark1-as3* cells treated or not with 10  $\mu$ M Napp1. Note that after Aurora inhibition, in a proportion of cells, centromeres are separated (Mis6 signal, left) but telomeres (Taz1 signal, left, or Pot1 signal, right) remain as clusters.

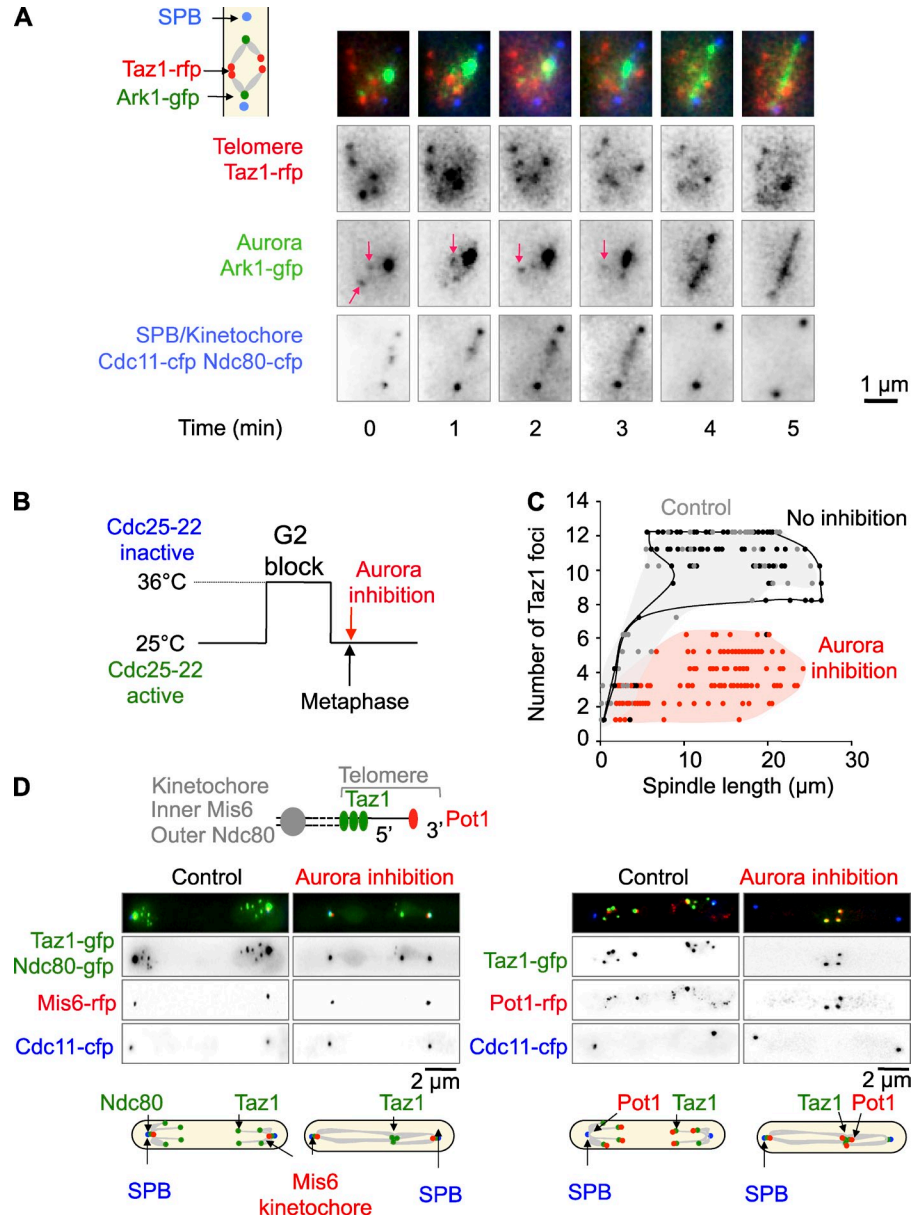


(Fig. 3 C, note the presence of telomere signals at the cell midzone). The spindle elongation rate was reduced ( $0.4 \pm 0.06 \mu\text{m}/\text{min}$ ; Fig. 3, A and B, green) and spindles often collapsed (Fig. S3 A). Eventually, cell death occurred after cell abscission (Fig. S3 B), similarly to the so-called cut phenotype (the formation of the septum between daughter cells in the absence of normal nuclear division; Hirano et al., 1986). Thus, telomere nondisjunction and/or defects in chromosome arm separation can impact mitotic progression independently of merotelic attachment.

Monopolin is a kinetochore protein that promotes kinetochore microtubule orientation in mitosis (and in meiosis I) and maintains rDNA integrity (Tóth et al., 2000; Poon and Mekhail, 2011). Deletion of the monopolin complex subunit Pcs1 in *S. pombe* results in merotelic attachments (Corbett et al., 2010; Rumpf et al., 2010; Gregan et al., 2011). We also observed a high frequency of chromosome attachment defects (including merotelic attachment) in *pcs1Δ* cells (Fig. 3 D, dark

gray or white bars) but, unlike Aurora inhibition, no defects in telomere disjunction (Fig. 3 D, light gray bars). Together, these experiments reveal that telomere nondisjunction and/or chromosome arm separation defects mechanically block chromosome segregation and lead to the formation of anaphase chromatin bridges independently of merotelic attachment.

#### The role of Aurora B in telomere dispersion is Rap1 independent but Swi6/HP1 dependent

In fission yeast, Taz1 binds to double-stranded telomere DNA (Cooper et al., 1997) and recruits Rap1. Rap1 is part of the shelterin complex that protects chromosome ends and telomere length in a Taz1-dependent manner (Cooper et al., 1998; Chikashige and Hiraoka, 2001; Ferreira and Cooper, 2001; Kanoh and Ishikawa, 2001; Kanoh et al., 2005; Miller et al., 2005). Recent investigation suggests that Rap1 phosphorylation by the Cdk1 kinase (Cdc2) induces telomere dissociation



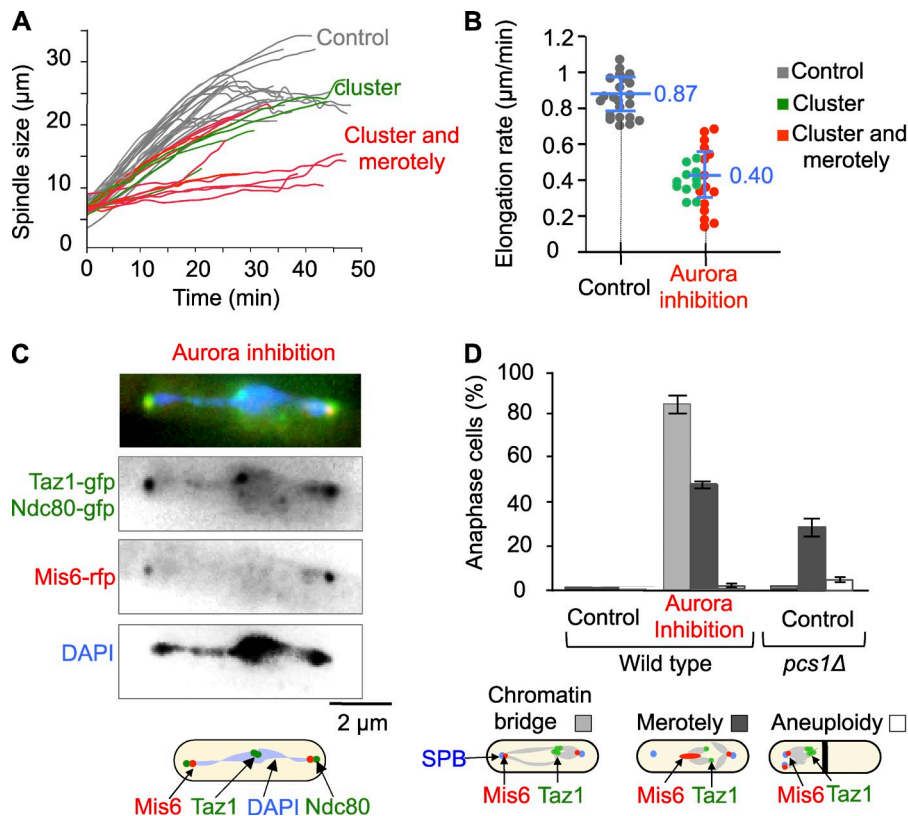


**Figure 3. Telomere nondisjunction mechanically disturbs spindle elongation and leads to the formation of anaphase chromatin bridges.** (A) Single cell analysis of spindle elongation during mitotic progression in the absence (gray lines,  $n = 22$ ) or in the presence of  $10 \mu\text{m}$  Napp1 (red,  $n = 13$ , and green,  $n = 4$  lines). In the presence of  $10 \mu\text{m}$  Napp1, cells displaying telomere segregation defects and merotelic attachments are shown in red, whereas cells with telomere nondisjunction defects are shown in green. (B) Mean rate of spindle elongation for the different phenotypes shown in A. (C) Example of a fine chromatin bridge seen after Aurora inhibition with correctly segregated kinetochores. (D) Percentage of anaphase chromatin bridges, merotely, and aneuploidy phenotypes in control ( $n = 206$ ), after Aurora inhibition ( $n = 293$ ), or in cells deleted for the monopolin subunit Pcs1 ( $n = 221$ ). Light gray, anaphase bridges; dark gray, merotely; white, aneuploidy. Error bars indicate SD obtained from three independent experiments.

from the nuclear envelope (Fujita et al., 2012). We tested the role of Rap1 in telomere disjunction by single cell analysis before or after Aurora B inhibition using *ark1-as3 rap1* $\Delta$  cells (Fig. 4, A and B). The number of Taz1 foci were scored with respect to spindle length in *rap1* $\Delta$  cells with (Napp1; Fig. 4, A and B, red dots) or without Aurora inhibition (Fig. 4, A and B, control, black dots). Aurora inhibition blocked both telomere dispersion and disjunction (only up to four Taz1 dots) and nucleolar segregation (Fig. S2 B), suggesting that Aurora B controls telomere dispersion and disjunction in a Rap1-independent manner.

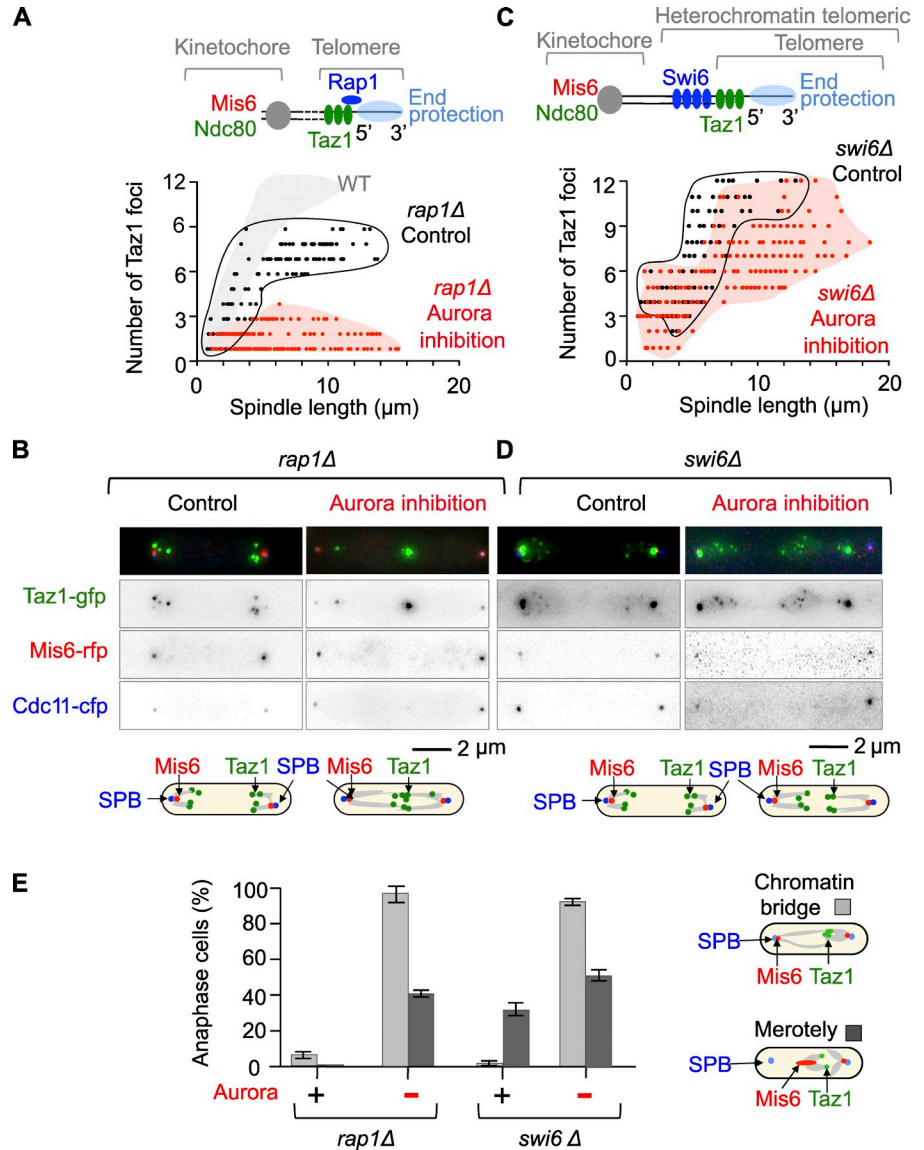
Telomere disjunction and nucleolar segregation were largely unaffected in the absence of Rap1. Indeed, we observed the presence of stretched telomeres in only 5% ( $n = 500$ ) of mitotic cells during anaphase, whereas the nucleolus and the kinetochores segregated normally (Fig. S4 A). In those cells showing stretched telomeres, spindle elongation was reduced to  $0.48 \pm 0.04 \mu\text{m}/\text{min}$ , demonstrating that sister telomere nondisjunction alone can affect spindle elongation (Fig. S4 B). Stretched telomeres eventually relaxed to single dots that moved to the spindle poles (Fig. S4 A). In addition to these rare telomere nondisjunction defects, we noticed a severe defect in telomere dispersion in *rap1* $\Delta$  cells. A maximum of 9 Taz1 dots were observed after full spindle elongation instead of the 12 dots in the wild type (Fig. 4 A, black dots). Statistical analysis of a population of *rap1* $\Delta$  cells in early anaphase (before telomere reclustering) confirmed that telomeres failed to fully separate (Fig. S4 C). Thus, telomere disjunction can be uncoupled from telomere dispersion, suggesting that independent mechanisms control these events.

The heterochromatin protein Swi6/HP1 localizes to telomeres, centromeres, and the mating type locus (Ekwall et al., 1995; Nakayama et al., 2001). To address the role of Swi6 in sister chromatid telomere disjunction, we performed single cell analysis in *ark1-as3 swi6* $\Delta$  cells (Fig. 4 C). The number of Taz1 foci were scored with respect to spindle length in *swi6* $\Delta$  cells with (Napp1; Fig. 4, C and D, red dots) or without Aurora inhibition (Fig. 4, C and D, control, black dots). Unlike *rap1* $\Delta$  or wild-type cells, telomere dispersion occurred more or less normally in *swi6* $\Delta$  cells after Aurora inhibition (Fig. 4, C and D, red dots; and Fig. S4 D), although these cells showed high levels of merotelic attachment (Fig. 4 E, dark gray bars). Further, telomere dispersion was not sufficient to promote telomere disjunction and nucleolar segregation after Aurora inhibition in *swi6* $\Delta$ . Rather, cells revealed decondensed chromosome arms, separated telomeres, and nonsegregated nucleoli, leading to anaphase chromatin bridges and cell death (Fig. 4 E, light gray bars; and Fig. S2 B). Finally, Swi6/HP1 deletion was sufficient to rescue the telomere dispersion defects of *rap1* $\Delta$  cells as shown by the increased number of foci per nuclei in the double mutant *rap1* $\Delta$  *swi6* $\Delta$  (Fig. S4 E). These experiments suggest that Aurora B controls telomere dispersion and disjunction through separate mechanisms and that telomere dispersion is Swi6/HP1 dependent.

#### Aurora B controls the dissociation of the cohesin Rad21 and Swi6/HP1 from telomeres at anaphase

Previous work has established that cohesin participates in subtelo-meric heterochromatin maintenance in fission yeast, probably

**Figure 4. The role of Aurora B in telomere disjunction is Rap1 independent but Swi6/HP1 dependent.** (A) Rap1-deleted cells were filmed through mitosis in the presence (Aurora inhibition, red,  $n = 139$ ) or absence (control, black,  $n = 111$ ) of  $10 \mu\text{M}$  Napp1 and the number of Taz1 dots was counted according to spindle length. Note that clusters do not fully dissociate in Rap1-deleted cells as compared with wild type (light gray in the graph). The data shown are from a single representative experiment out of three repeats. (B) Example of phenotypes seen in *ark1-as3 rap1 $\Delta$*  cells treated or not with  $10 \mu\text{M}$  Napp1. (C) Swi6-deleted cells were filmed through mitosis in the presence (Aurora inhibition, red,  $n = 127$ ) or absence (control, black,  $n = 70$ ) of  $10 \mu\text{M}$  Napp1 and the number of Taz1 dots was counted according to spindle length. The data shown are from a single representative experiment out of three repeats. (D) Example of phenotypes seen in *ark1-as3 swi6 $\Delta$*  cells treated or not with  $10 \mu\text{M}$  Napp1. (E) Percentage of anaphase chromatin bridges (light gray) and merotelly phenotype (dark gray) before or after Aurora inhibition in *rap1 $\Delta$*  or *swi6 $\Delta$*  cells. Light gray, anaphase bridges; dark gray, merotelly. Error bars indicate SD.



acting locally on Swi6/HP1 binding in the subtelomeric region (Nonaka et al., 2002; Dheur et al., 2011). To better understand the intricate relationship between Aurora B and its telomeric target, we analyzed the impact of Aurora inhibition on both cohesin Rad21 and Swi6/HP1 localization. We performed live imaging of *ark1-as3* cells simultaneously expressing Rad21-gfp (cohesin subunit) or Swi6-gfp (heterochromatin HP1) together with markers for the SPBs (Cdc11-cfp) and kinetochores (Mis6-rfp). In control cells, we observed that cohesin Rad21 concentrates into discrete foci in early mitosis, which disappear at anaphase onset (Fig. 5 A). These foci colocalize with telomere and centromere markers (unpublished data). When Aurora was inhibited in mitotic cells, Rad21 remained specifically associated with telomere foci, but not centromeres, after full spindle elongation (Fig. 5 A). Like Rad21, Swi6 localizes to telomeres and centromeres in interphase cells (Ekwall et al., 1995; Nakayama et al., 2001; Fig. 5 B and Fig. S5 A). In control cells, Swi6/HP1 transiently dissociates from telomeres during mitosis (Fig. 5 C, green line; and Fig. S5 B, red line), concomitantly with the increase in the rate of spindle elongation

(Figs. 5 C and S5 B, black line). This suggests that Swi6 removal occurs at the metaphase-to-anaphase transition (Fig. 5 C). Subsequently, Swi6 progressively reappears at the telomeres during anaphase B (Fig. 5, B–D; and Fig. S5, A and B) and remains so in G2 (Fig. 5 C, blue line) or when Aurora is inhibited in mitotic cells, even after full spindle elongation (Fig. 5, B–D). This transient dissociation of Swi6/HP1 from the telomeres in mitosis was confirmed by analysis of multiple cells (Fig. 5 D). Finally, we found that the cohesin Rad21 was not with telomeres in *swi6 $\Delta$*  cells even after Aurora inhibition (Fig. S5 C). Together, these experiments suggest that Aurora-dependent removal of Swi6/HP1 and consequently cohesin Rad21 from telomeres in early mitosis contributes to telomere dispersion.

#### Aurora B-dependent phosphorylation of condensin bypasses telomere nondisjunction in mitosis

To clarify the mechanisms leading to Aurora B-dependent telomere disjunction, we tested several key players in chromosome segregation. Recent studies in fission yeast have established that

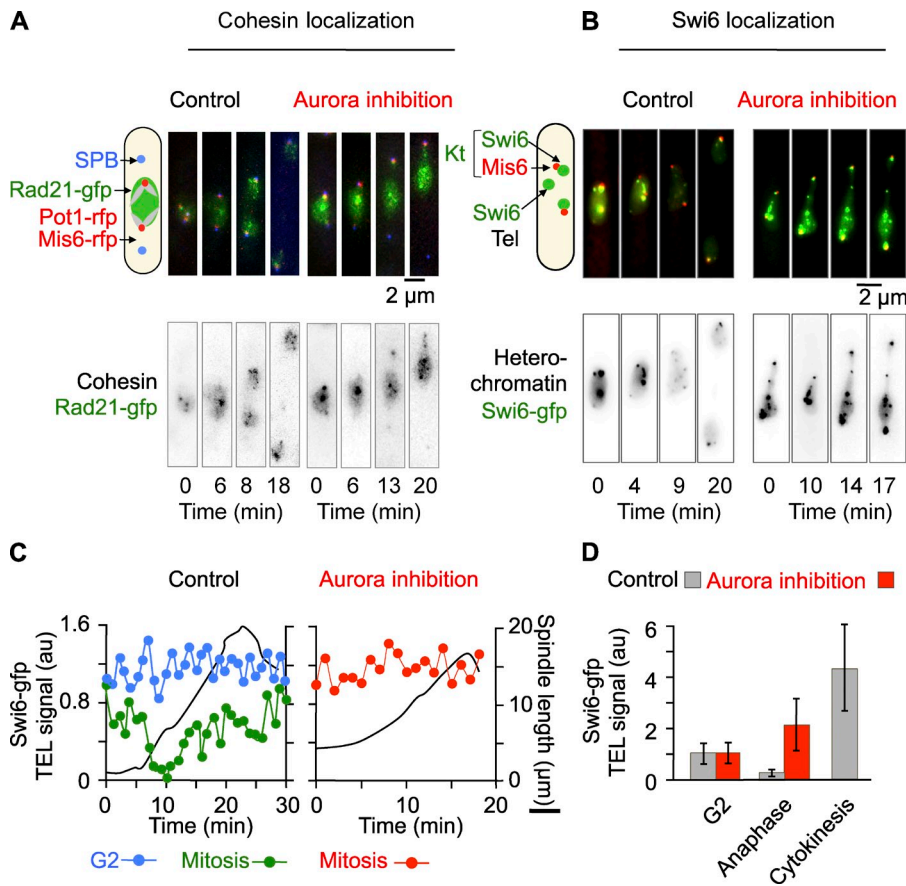


**Figure 5. Aurora B controls the dissociation of cohesin Rad21 and Swi6/HP1 from telomeres at anaphase.** (A) *Rad21-gfp mis6-rfp pot1-rfp ark1-as3* cells were filmed through mitosis in the presence (Aurora inhibition, red) or absence (control, black) of 10  $\mu$ M Napp1. Rad21 remains associated to telomeres as judged by its colocalization with the telomeric Pot1 signal after Aurora inhibition. (B) *swi6-gfp mis6-rfp ark1-as3* cells were filmed through mitosis in the presence (Aurora inhibition, red) or absence (control, black) of 10  $\mu$ M Napp1. (C) Quantification of the normalized mean fluorescence intensity of Swi6-gfp at telomeres during mitotic progression as a function of spindle length (in black) in the cells shown in A. In control mitotic cells (green), the decrease in Swi6-gfp is concomitant to the increase in spindle length during anaphase onset (black). During anaphase B, Swi6-gfp progressively reaccumulates at telomeres. In the presence of Napp1 (Aurora inhibition, red), Swi6-gfp remains constant at telomeres during spindle elongation (in black). The intensity of Swi6-gfp at telomeres in G2 cells simultaneously filmed within the same field of cells than in A is shown as a control (blue). Multiple cells were analyzed and behave in a similar manner. (D) Statistical analysis showing the mean intensity of Swi6-gfp signal at telomeres as a function of the cell cycle stage (G2, anaphase, or cytokinesis) in the presence (red) or absence (gray) of Napp1. Error bars indicate SD.

a condensin subunit (Cnd2) is an Aurora B substrate (Nakazawa et al., 2011; Tada et al., 2011). A condensin phosphomimetic mutant (*cnd2-3E*) alleviates the chromosome segregation defects in cells where Aurora B has been inactivated (Nakazawa et al., 2011; Tada et al., 2011). Hence, condensin may be the essential target of Aurora B at the fission yeast kinetochore. We speculated that phosphorylation of Cnd2 by Aurora B may also be sufficient to promote telomere dispersion or disjunction. To address this point, we used *cnd2-3E ark1-as3* mutant cells that also expressed SPB (Cdc11-cfp), kinetochore (Ndc80-gfp and Mis6-rfp), and telomere (Taz1-gfp) markers. We scored the number of Taz1 foci relative to spindle length in wild-type or *cnd2-3E* cells after Aurora inhibition (Fig. 6 A, red dots). We found that the *cnd2-3E* mutant partially bypassed the telomere nondisjunction effects imposed by Aurora inhibition (Fig. 6, A and B; and Fig. S5 D) and was also able to rescue nucleolar segregation in  $75.6 \pm 3.2\%$  ( $n = 97$ ) of cells observed (Fig. S2 B).

However, although in wild-type cells telomere dispersion was initiated in phases 1 and 2, before telomere disjunction (Fig. 1, C and D; and Fig. 6, C and D), *cnd2-3E* mutant undergoes telomere disjunction in the absence of full dispersion after Aurora inhibition. An example of this is shown by single cell analysis in Fig. 6 (C and D), together with a quantification of Taz1 foci during spindle elongation. Conversely, telomere disjunction defects were observed in a phospho-null mutant of Cnd2 (*cnd2-3A*) even after full spindle elongation (Fig. 6 B, right). Dispersion seems to occur normally in *cnd2-3A*, which remains viable, as opposed to Aurora inhibition (Fig. 6 B, right).

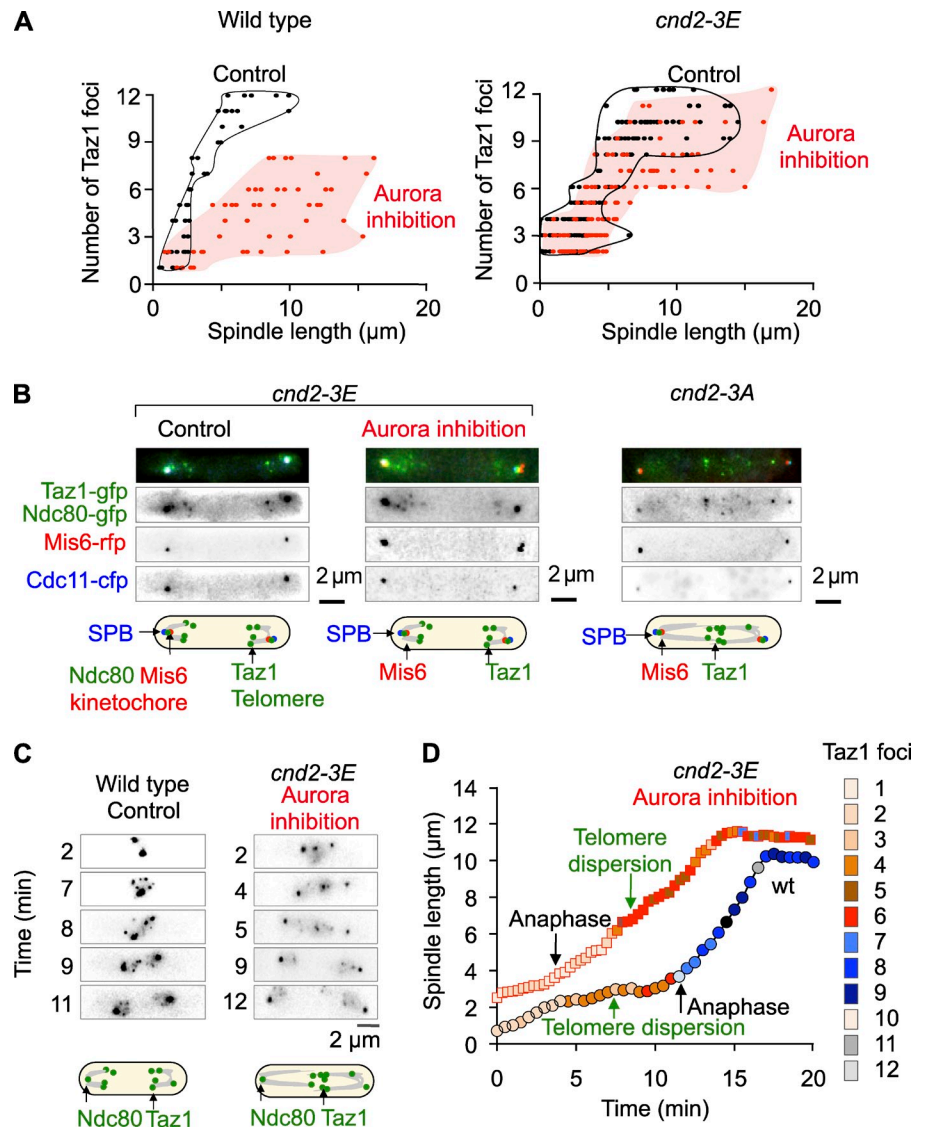
These observations suggest that Aurora B controls telomere disjunction through condensin phosphorylation but that telomere dispersion is independent of condensin.

### The role of Aurora B in telomere dispersion and disjunction requires the shelterin component Ccq1

Our results suggest that Aurora B may play a specific role at telomeres to participate in chromosome arm separation. Chromosome ends are capped by a protein complex known as shelterin (de Lange, 2009; Nandakumar and Cech, 2013). In fission yeast, one of the proteins of this complex, Ccq1, is required for telomerase recruitment. Because telomere length is reduced in *ccq1* $\Delta$  cells, chromosomes undergo circularization after several rounds of division and display DNA damage phenotypes (elongated cells and G2 delays; Tomita and Cooper, 2008). To select a population of *ccq1* $\Delta$  cells with noncircular chromosomes and no chromatin bridges, experiments were performed rapidly after strain selection (see Material and methods). At this early stage, *ccq1* $\Delta$  cells still exhibit telomeric Taz1 and normal cell size. We addressed the role of Ccq1 in sister chromatid telomere disjunction by performing single cell analysis in a population of *ark1-as3 ccq1* $\Delta$  cells (Fig. 7, A and B). Taz1 foci were scored with respect to spindle length with (Napp1; Fig. 7, A and B, red dots) or without Aurora inhibition (control, black dots). Telomere dispersion occurred in a majority of cells deleted for Ccq1 and the Aurora-dependent nondisjunction defects were partially rescued (Fig. 7, A–C, red dots). Statistical analysis revealed that



Figure 6. **Aurora B-dependent phosphorylation of condensin bypasses telomere nondisjunction but not dispersion.** (A) Wild-type or the phosphomimetic mutant *cmd2-3E* cells were filmed through mitosis in the presence (Aurora inhibition, red,  $n = 48$  control;  $n = 110$  *cmd2-3E*) or absence (control, black,  $n = 42$  control;  $n = 92$  *cmd2-3E*) of  $10 \mu\text{M}$  Napp1 and the number of Taz1 dots was counted according to spindle length. The data shown are from a single representative experiment out of three repeats. (B) Example of phenotypes seen in *cmd2-3E ark1-as3* or *cmd2-3A ark1-as3* cells treated or not with  $10 \mu\text{M}$  Napp1. (C) Example of a wild-type cell control and a *cmd2-3E ark1-as3* with Napp1 during mitotic progression. (D) The number of Taz1 foci (color code shown on the right) according to spindle length is analyzed from the movies shown in C. Note that in control cells (circles), telomere dispersion occurs before anaphase as opposed to *cmd2-3E* cells (squares) in the presence of Aurora inhibitor. Multiple cells were analyzed and display defects in telomere dispersion.



both *ccq1* deletion and the condensin *cmd2-3E* phosphomimetic mutant rescued to some extent the formation of anaphase chromatin bridges (Fig. 7 C, light gray bars). In the condensin mutant, the rescue was not specific to chromosome arm segregation defects as the appearance of merotelic attachment after Aurora inhibition was also bypassed. Instead, deletion of Ccq1 specifically reduced the appearance of anaphase chromatin bridges but not kinetochore attachment defects (Fig. 7 C, dark gray bars).

Finally, the *cmd2-3A* strain showed a high percentage of anaphase chromatin bridges but few merotelic attachments (Fig. 7 C). In agreement with these findings, both condensin phosphomimetic mutant and *ccq1* deletion rescued cell viability after Aurora inhibition (Fig. 7 D) and also bypassed the defect in nucleolar segregation (not depicted).

#### Deletion of Ccq1 rescues cell death after Aurora inhibition by promoting the loading of condensin onto chromosome arms

In fission yeast, Aurora B-dependent phosphorylation of the kleisin Cnd2 promotes condensin recruitment to chromosomes

(Nakazawa et al., 2011; Tada et al., 2011). To clarify how Ccq1 deletion rescued Aurora inhibition, we performed single cell analysis of condensin (*cmd1-gfp*) recruitment on chromosomes during mitosis in control cells, *ccq1Δ* cells, and phosphomimetic *cmd2-3E* mutant. As previously described, condensin colocalizes to several nuclear compartments during mitosis (Nakazawa et al., 2008), including the nucleolus (rDNA) and kinetochores. At anaphase onset, condensin localization switches to chromosome arms (Fig. 8 D, bottom, Hoechst) and the spindle midzone (Fig. 8, B and D). Transient localization of condensin with telomere clusters was also occasionally observed during metaphase (Fig. 8 D). In *ccq1Δ* cells and *cmd2-3E* mutant, this mitotic pattern of condensin localization was unchanged (Fig. 8, C and E, top). However, we noted that although Pot1 decreased in mitosis in control and *ccq1Δ* cells, it remained strongly associated with telomeres in the *cmd2-3E* mutant.

The effect of Aurora inhibition on condensin dynamics was investigated (Fig. 8, B, C, and E, Aurora inhibition). In wild-type cells, condensin recruitment to chromosome arms in



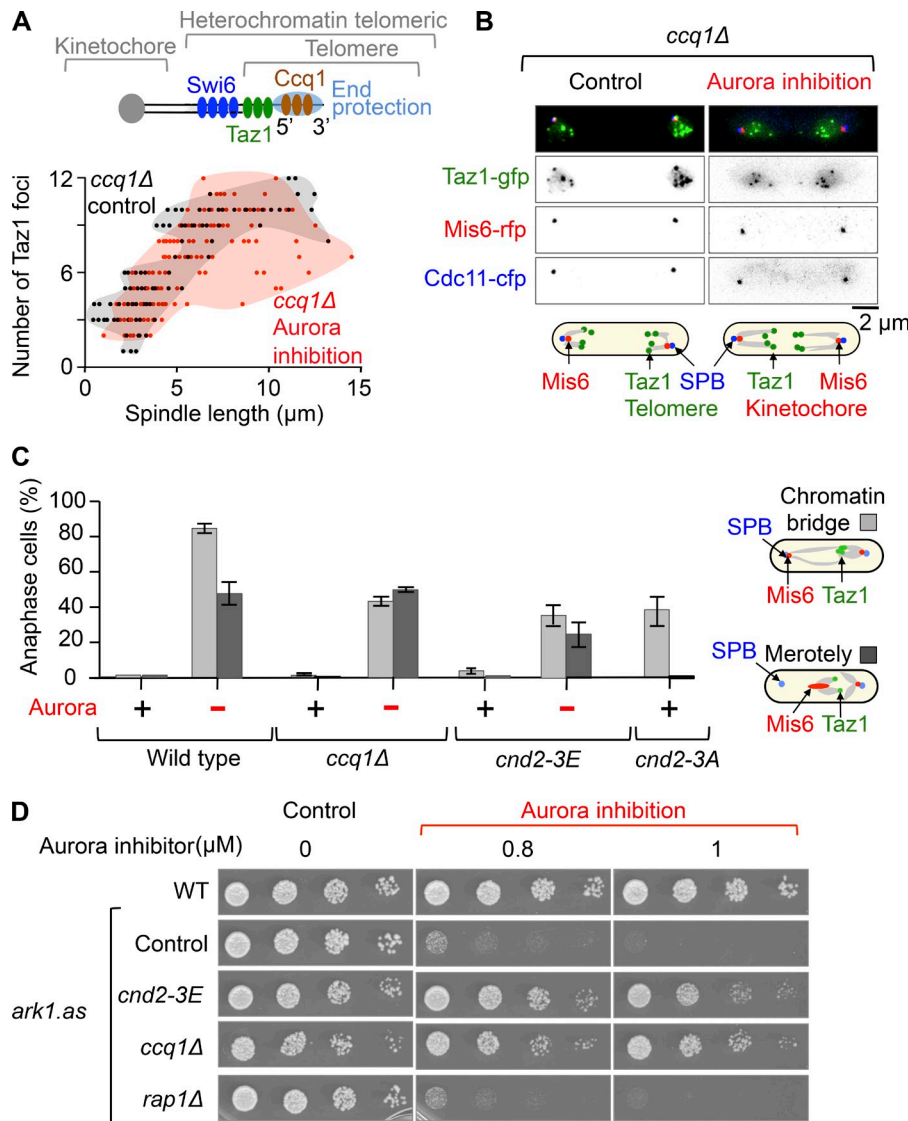


**Figure 7. The role of Aurora B in telomere dispersion and disjunction requires the shelterin component Ccq1.** (A) *Ccq1*-deleted cells were filmed through mitosis in the presence (Aurora inhibition, red,  $n = 92$ ) or absence (control, black,  $n = 79$ ) of  $10 \mu\text{M}$  Napp1 and the number of Taz1 dots was counted according to spindle length. The data shown are from a single representative experiment out of three repeats. (B) Example of phenotypes seen in *ark1-as3 ccq1\Delta* cells treated or not with  $10 \mu\text{M}$  Napp1. (C) Percentage of anaphase chromatin bridges and merotely phenotype before or after Aurora inhibition in *ccq1\Delta* ( $n = 210$ ), *cnd2-3E* ( $n = 250$ ), or *cnd2-3A* ( $n = 46$ ) cells. Light gray, anaphase bridges; dark gray, merotely. Error bars indicate SD. (D) Sensitivity of wild-type, *ccq1\Delta*, *rap1\Delta*, and *cnd2-3E* mutant cells to low doses of Napp1 ( $0.8 \mu\text{M}$  or  $1 \mu\text{M}$ ) was evaluated after serial dilutions of cells on plates. Note that under these conditions *ccq1\Delta* or *cnd2-3E* cells survive as opposed to wild type.

anaphase was clearly reduced after Aurora inhibition (Fig. 8 B, bottom, arrows; Nakazawa et al., 2011; Tada et al., 2011). Conversely, condensin remained correctly loaded on chromosome arms in the absence of Ccq1 or in the phosphomimetic mutant *cnd2-3E* after Aurora inhibition (Fig. 8, C and E, bottom, arrows). Together these experiments suggest that Aurora plays a specific role at telomeres to promote telomere dispersion and disjunction and that this mechanism contributes to correct condensin loading and chromosome arm separation.

## Discussion

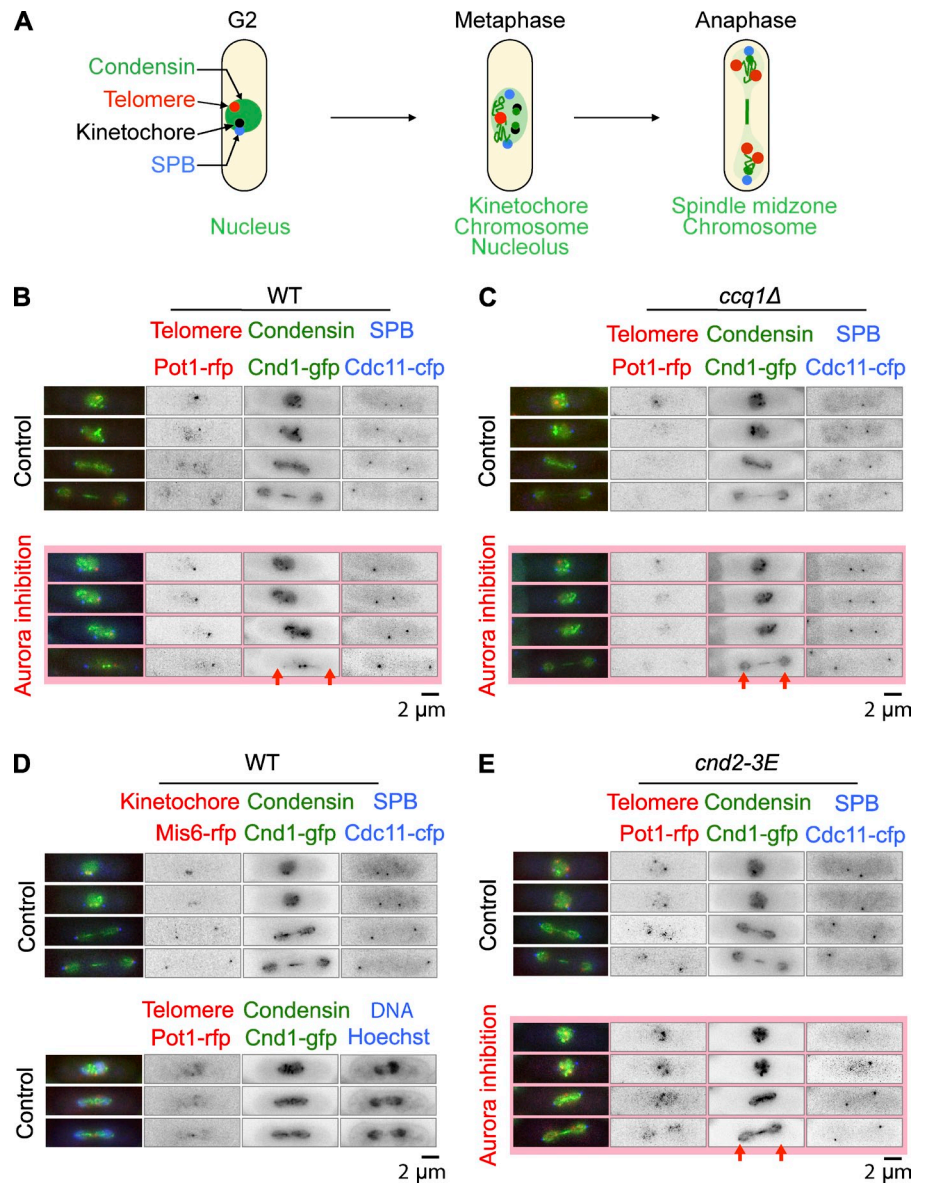
Our study demonstrates that the physical association of telomeres is tightly cell cycle regulated. During mitosis, telomere foci first dissociate from the nuclear envelope (Fujita et al., 2012) and then undergo separation in two discrete steps. Telomere dispersion (up to six dots) occurs during metaphase, before chromosome segregation, whereas sister chromatid telomere disjunction (up to 12 dots) is achieved during mid-anaphase. Aurora B is required for both steps but not for telomere

dissociation from the nuclear envelope (unpublished data). Our findings are thus not related to previous studies describing an important role for telomere dissociation from the nuclear envelope in the control of chromosome arm separation (Fujita et al., 2012; Titos et al., 2014).

We demonstrate that Aurora B targets spatially distinct heterochromatin domains, centromeres, and telomeres to control chromosome segregation. Interestingly, Aurora localization to telomeres is both Bub1 and Swi6 independent (unpublished data). These findings are in agreement with previous work performed by chromatin immunoprecipitation on the CPC component Bir1 (Yamagishi et al., 2010). Other studies have reported that the Shugoshin protein Sgo2 is required for the proper recruitment of Aurora at centromeres (Hauf et al., 2007; Vanoosthuyse et al., 2007). We found that the CPC was still able to localize to both centromeres and telomeres in the absence of Sgo2 although the signal was somewhat reduced. As expected, *sgo2\Delta* cells are not defective in telomere disjunction, show very few merotelic attachments, and are viable, phenotypes not observed in Aurora-depleted cells (unpublished data).

**Figure 8. Deletion of Ccq1 rescues cell death after Aurora inhibition by promoting the loading of condensin on chromosome arms.**

(A) Schematic representation illustrating the different localization of condensin throughout mitosis. (B) Single cell analysis of *ark1-as pot1-rfp cnd1-gfp cdc11-cfp* cells imaged in the presence or absence of 10  $\mu$ M Napp1 (Aurora B inhibition). (C) Single cell analysis of *ccq1 $\Delta$  ark1-as pot1-rfp cnd1-gfp cdc11-cfp* cells imaged in the presence or absence of 10  $\mu$ M Napp1 (Aurora B inhibition). (D) Single cell analysis of *ark1-as mis6-rfp cnd1-gfp cdc11-cfp* or *ark1-as pot1-rfp cnd1-gfp cdc11-cfp* cells imaged in the presence or absence of 10  $\mu$ M Napp1. In B, C, and E, the red arrows highlight the presence or absence of condensin localization to chromosome arms.



In addition to its role in kinetochore–microtubule attachment, Aurora B promotes the transient dissociation of Swi6/HP1 from the telomeres at the metaphase-to-anaphase transition. This event likely contributes to telomere dispersion, as the cohesin subunit Rad21 also remains strongly associated with telomere clusters in a Swi6-dependent manner. In contrast, Rad21 is not retained on chromosome arms and this observation is also confirmed by chromatin immunoprecipitation data indicating that Rad21 is specifically lost from heterochromatic sites but not other sites on chromosome arms in *swi6 $\Delta$*  cells (Bernard et al., 2001; Nonaka et al., 2002). Hence, the absence of telomeric heterochromatin (Swi6/HP1 deletion) is sufficient to bypass the telomere dispersion defects seen after Aurora inhibition or after deletion of Rap1.

Chromosome end protection in *S. pombe* is similar to that seen in mammals and a recent study has identified several proteins including Pot1 or Ccq1 that form the shelterin complex (Miyoshi et al., 2008). Ccq1 is the *S. pombe*-specific component of this complex and is required for telomerase recruitment

(Moser et al., 2011; Yamazaki et al., 2012). Ccq1 also participates in the telomeric recruitment of a multi-enzyme complex (termed SHREC) that mediates heterochromatic transcriptional gene silencing (Sugiyama et al., 2007). The dissociation of shelterin components from telomeres during mitosis was previously demonstrated using chromatin immunoprecipitation (Chang et al., 2013). Our study provides the timing for this dissociation with respect to chromosome segregation and telomere dispersion. It also suggests that Aurora controls the dissociation of Pot1 or Ccq1 at the metaphase-to-anaphase transition (Fig. 9).

In parallel to its role in dissociating Swi6/HP1, Pot1, or Ccq1 from telomeres and promoting telomere dispersion, Aurora B promotes chromosome arm separation by phosphorylating the condensin subunit Cnd2 (Nakazawa et al., 2011; Tada et al., 2011). Condensins are universal organizers of chromosomes that participate in several processes, such as condensation and segregation of rDNA, clustering of tRNA genes, axial compaction of pericentric chromatin, and recoiling of stretched

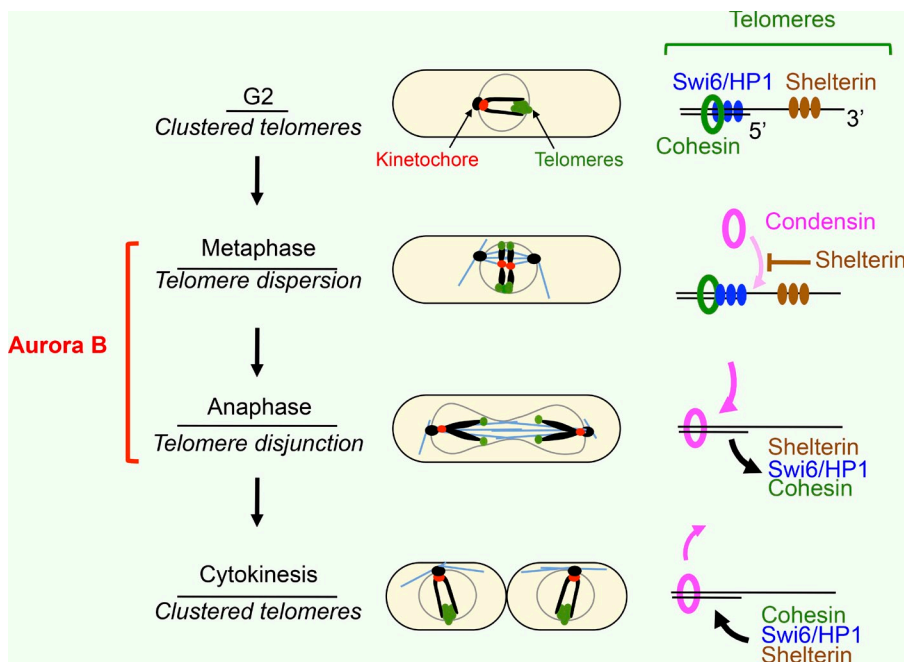


Figure 9. **Model summarizing the different state in telomere clustering throughout mitosis.** Schematic representation illustrating the regulation of telomere dissociation throughout mitosis. (left) Telomere foci undergo separation in two discrete steps. Telomere cluster dispersion (up to 6 dots) occurs during metaphase, before chromosome segregation, whereas sister chromatid telomere disjunction (up to 12 dots) is achieved during mid-anaphase. Finally, telomere reclustering occurs during cytokinesis (subsequent G1/S phase). Aurora B is required for telomere dispersion and disjunction. (right) At the level of telomeres, Aurora promotes in metaphase the delocalization of several telomere/subtelomere components, such as shelterin components (brown), Swi6/HP1 (blue), or cohesin Rad21 (green). At anaphase, Aurora favors the loading of condensin (pink). Our model suggests that the delocalization of telomere components such as the shelterin protein Ccq1 promotes telomere dispersion and Aurora-dependent loading of condensin to chromosome arms.

chromosome arms in anaphase (Carmena et al., 2012). Our study shows that a phosphomimetic mutant of the condensin subunit Cnd2 (*cnd2-3E*) is unable to rescue the telomere dispersion defects seen after Aurora inhibition. Our study therefore suggests that telomere dispersion is promoted by a separate mechanism involving the removal of Swi6/HP1. Rather, condensin controls telomere disjunction and nucleolar segregation by mechanically pulling on chromosome arms. In agreement with this model, Swi6/HP1 and Pot1 remain associated with telomeres when Aurora is inhibited in a *cnd2-3E* mutant even after telomere disjunction. In addition, the condensin mutant *cut3* arrests with dispersed telomeres (up to six dots) but nonseparated chromosome arms (unpublished data).

The removal of Swi6/HP1 from heterochromatin in mitosis has been observed in several organisms. Whereas in higher eukaryotes the biological significance of this event remains to be determined, in budding yeast Aurora B-dependent phosphorylation of H3S10 is thought to contribute to chromosome compaction during anaphase (Neurohr et al., 2011). This modification causes the removal of HP1/Swi6 from H3K9me3, which facilitates the dissociation of the CPC from chromosome arms and its enrichment at centromeres (Nozawa et al., 2010). In fission yeast, Aurora B also controls the phosphorylation of histone H3 on Serine 10 (Petersen et al., 2001) and the removal of Swi6/HP1 from telomeres (Chen et al., 2008; this study). Whether or not this pathway is responsible for telomere separation in fission yeast is currently unknown.

It is tempting to speculate that the different states of telomere clustering observed during the fission yeast cell cycle reflects the dynamics of cohesion at telomeres. Indeed, a recent study established that cohesin participates in subtelomeric heterochromatin maintenance in fission yeast, probably by acting locally on Swi6/HP1 binding in the subtelomeric region (Dheur et al., 2011). In agreement with this hypothesis, neither *rad21-K1* cohesin mutant nor the *swi6Δ* mutant show correct telomere

clustering in interphase fission yeast cells (unpublished data) and Rad21 is maintained at telomeres when Aurora is inhibited. If this is the case, the initial step in cluster dissociation in metaphase cells may be reminiscent of the prophase dissociation pathway that is seen in higher eukaryotes (Waizenegger et al., 2000). Intriguingly, it has been shown that two pathways are required to dissociate cohesin from chromosomes in such cells. The first, in prophase, requires the activity of Aurora B and polo-like kinase (Losada et al., 2002; Sumara et al., 2002; Giménez-Abián et al., 2004), whereas the second requires the proteins Wapl and Pds5 (Gandhi et al., 2006; Kueng et al., 2006; Shintomi and Hirano, 2009). Further experiments will be required to establish whether telomere dispersion in mitosis in fission yeast is homologous to the prophase dissolution pathway seen elsewhere.

Our work raises the following important question: what are the respective roles for telomere dispersion and disjunction in chromosome segregation? When Aurora B is inactivated, sister chromatids are entangled along the chromosome arms, including the telomere-adjacent regions. Thus, telomere nondisjunction might be an indirect effect of arm nondisjunction. However, because the telomere-specific component Ccq1 is required for telomere nondisjunction and for cell viability after Aurora inhibition, we propose that the dissociation of the shelterin complex in early mitosis initiates telomere dispersion, promotes condensin loading, and participates to chromosome arm separation. How Ccq1 deletion triggers condensin loading and chromosome arm separation after Aurora inhibition remains to be determined but a more thorough examination of CPC function in Ccq1-deleted cells should shed light on such questions.

One source of mitotic instability is the presence of chromosomes with dysfunctional telomeres. This defect could give rise to chromatin bridges at anaphase, leading to chromatin fragmentation or chromosome loss (Gisselsson and Höglund, 2005). Our study reveals a novel mechanism that controls



chromosome segregation, which requires telomere integrity independently of the segregation of other heterochromatin loci such as centromeres.

## Materials and methods

### Cell culture

Media, growth, maintenance of strains, and genetic methods were as described previously (Moreno et al., 1991). Cells were grown at 25°C in yeast extract and centrifuged 30 s at 3,000 g before mounting onto an imaging chamber. All strains used in the study were isogenic to wild-type 972 and are listed in Table S1. Strains from genetic crosses were selected by random spore or tetrad dissection and selected in the presence of appropriate supplements or drugs, or screened visually for the presence of the appropriate fluorescent markers. Visualization of the nucleolus was achieved by the expression of the plasmid pREP41x/fib1-mRFP (Beauregard et al., 2009). Yeast transformations were performed by electroporation in the presence of thiamine (repressive condition). Fib1-mRFP protein was induced by growing the cells in the absence of thiamine for 24 h. For Aurora inhibition rescue, *ccq1Δ* colonies were taken at an early stage of selection before chromosome circularization (as judged by the lack of sensitivity to methyl methanesulfonate). At this early stage (between 2 to 7 d of growth), Taz1 signal was still observed and cell size was comparable to wild type. *Ccq1Δ* colonies with circular chromosomes (as judged by sensitivity to methyl methanesulfonate) did not rescue Aurora inhibition. The presence of different types of colonies in *ccq1Δ* or *tpz1* mutants has been previously characterized (Harland et al., 2014).

### Mutant and tagged strains

Standard genetic and PCR-based gene targeting methods were used to construct *S. pombe* strains (Table S1). All fluorescently tagged (*gfp*, *rfp*, and *cfp*) and truncated genes (full-length truncations) are under the control of their endogenous promoters and integrated at their native chromosomal loci. Most of the deleted or epitope-tagged strains were thus produced by homologous recombination using modified pFA6a series of plasmids carrying hygromycin-resistance gene (*hyg* in strain list; Hentges et al., 2005) or previously described pFA6a series of plasmids carrying kanamycin-resistance gene (*kanR* in strain list; Bähler et al., 1998). This includes *taz1-gfp* (gift from J. Cooper, Center for Cancer Research, National Institutes of Health, Bethesda, MD), *amo1-rfp* (gift from P. Nurse, Cancer Research UK, London, England, UK), *mis6-2rfp* (gift from T. Toda, Cancer Research UK, London, England, UK), *ndc80-gfp cdc11-cfp* (Tournier et al., 2004), *taz1-mrfp* and *ccq1Δ* (gift from M. Flory, Wesleyan University, Middletown, CT; Motwani et al., 2010), *rad21-gfp* (gift from J.P. Javerzat, Institut de Biochimie et Genetique Cellulaires, Bordeaux, France, and P. Bernard, Université Claude Bernard Lyon 1, Lyon, France), *pot1-rfp* (gift from V. Geli, Centre de Recherche en Cancérologie de Marseille, Marseille, France), and *Cnd1-gfp* (gift from M. Yanagida, Osaka University, Osaka, Japan).

The *cnd1-gfp* strain is a full-length fusion created by homologous recombination and integrated at its native chromosomal loci (Sutani et al., 1999). The following deletions are full-length deletions created by homologous recombination: *rap1::ura4* (gift from J. Kanoh, Institute for protein research, Osaka University, Osaka, Japan) and *swi6::his1 and pcs1::ura4* (gift from J.P. Javerzat).

The temperature-sensitive *cdc25-22* allele (Thuriaux et al., 1980) was used for fission yeast synchronization in G2 (<http://www.pombase.org/spombe/result/SPAC24H6.05>).

Fibrillarin fused with the mRFP (R.Y. Tsien, University of California, San Diego, La Jolla, CA) was constructed in two steps (Beauregard et al., 2009). First, mRFP was amplified using a pair of oligonucleotides: mRFP1-forw2 containing a XhoI restriction site and a PmeI restriction site (bold; 5'-CCGCTC-GAGGTTAAACGCCTCTCCGA-3'), and mRFP1-reverse, containing a BamHI site (5'-CGGGATCCTTAGCGCCGGTGGAGTG-3'). Subsequently, the PCR product was digested with XhoI and BamHI and cloned in pREP41X. Fibrillarin was amplified from genomic DNA with Fib1-XhoI forward (XhoI site; 5'-AGACTCGAGATGGCATATACACCAGGTTCA-3') and Fib1-PmeI-no-stop reverse (PmeI site in bold characters; 5'-AGAGTTAAACCCCTGATGTCACAG-TATTTCTAC-3'). After which, the PCR product was digested with XhoI and PmeI and inserted into pREP41X-mRFP, previously digested with the same enzymes (gift from L.A. Rokeach, Montreal University, Montreal, Canada).

The *cnd2-3A* strain (gift from Y. Watanabe, University of Tokyo, Tokyo, Japan) was created by changing S5, S41, and S52 to alanines and the genomic fragments carrying the mutations were transformed into

*Cnd2*-deleted cells (Tada et al., 2011). The integration at *cnd2::ura4* locus was selected by 5-fluoroorotic acid resistance and confirmed by PCR. A similar technique was used to construct the *cnd2-3E* strain (Tada et al., 2011).

The *ark1-as3* strain was created from *ark1-as2* by additionally mutating Ser229 to Ala (gift from S. Hauf, Virginia Polytechnic Institute and State University, Blacksburg, VA). To generate the *ark1-as2* allele (*Ark1-Leu166Ala*), the *ark1* gene was PCR mutagenized from a strain into which a hygromycin-resistance cassette (*hygR*) had been integrated 400 bp 5' of the *ark1+* open reading frame (Hauf et al., 2007). The *hygR-ark1-as2* construct was integrated in a wild-type strain at the endogenous locus. Both the *ark1-as2* and the *ark1-as3* strains contain the additional amino acid mutations Gln28Arg and Gln176Arg, which were unintentionally inserted during the first PCR mutagenesis (Hauf et al., 2007). Both alleles displayed sensitivity to the ATP analogue Napp1.

### Aurora inhibition

Aurora inhibition was performed using analogue-sensitive alleles of Ark1 (*ark1-as3*), which allows rapid and specific inactivation of Aurora kinase using the ATP analogue Napp1 (Hauf et al., 2007). As specified in the figure legends, asynchronous or synchronous populations of cells were filmed in the presence of 10 μM Napp1 and followed through mitosis. To quantify the mitotic defects seen after Aurora inhibition, the temperature-sensitive double mutant *cdc25-22 ark1-as3* was synchronized by incubation at 36°C to accumulate cells in G2 phase, and then released into early mitosis by incubation at the permissive temperature of 25°C (>80% of cells in phase 1) and adding 10 μM Napp1. Progress of the cells through mitosis was followed and attachment defects in anaphase were quantified by live cell imaging.

### Live cell imaging

Live cell analysis was performed in an imaging chamber (CoverWell PCI-2.5; Grace Bio-Labs) filled with 1 ml of 1% agarose in minimal medium and sealed with a 22 × 22-mm glass coverslip. Time-lapse images of Z stacks (maximum five stacks of 0.3–0.4-μm steps, to avoid photobleaching) were taken at 15-s intervals or as indicated in the relevant figure legend. Exposure times were 300–500 ms with a HiGHlite light source (Roper Scientific) reduced to 30% to avoid photo toxicity and photobleaching. Either the image with the best focal plane or projected images were prepared for each time point. Images were visualized with a charge coupled device CoolSNAP HQ camera (Roper Scientific) fitted to a DM6000 upright microscope (Leica) with a 100× (1.4 NA) objective and SEMROCK filters and were recorded using the MetaMorph software package (Molecular Devices). Intensity adjustments were made using the MetaMorph, ImageJ, and Adobe Photoshop packages (Adobe Systems).

### Analysis of spindle elongation and kinetochore misattachments

The position of the SPBs, kinetochores, and telomeres was determined by visualization of the *Cdc11-cfp*, *Ndc80-gfp/Mis6-rfp*, and *Taz1/Pot1* signals and captured using MetaMorph. Maximum intensity projections were prepared for each time point, with the images from each channel being combined into a single RGB image. These images were cropped around the cell of interest, and optional contrast enhancement was performed in MetaMorph where necessary. The cropped images were exported to IGOR (version Pro6; WaveMetrics) as 8-bit RGB-stacked TIFF files with each frame corresponding to one image of the time-lapse series. For both channels, custom peak detection was performed. The successive positions of the SPBs and kinetochores were determined. The data generated were used to calculate the rate of spindle elongation and the number of lagging kinetochores and telomeres. A merotelic kinetochore is defined as a single kinetochore (*Ndc80-gfp*) within an anaphase spindle that undergoes splitting while a corresponding single centromeric signal (*Mis6-rfp*) remains barely unstretched (Courthouex et al., 2009; Gay et al., 2012). Thus, imaging these two kinetochore and centromere markers simultaneously allows us to discriminate between merotelic attachment or lagging chromosomes attached to a single pole.

### Cell fixation

To determine the percentage of aneuploidy and cut phenotype, cells were fixed in 3.7% formaldehyde for 7 min at room temperature, washed once in PBS, and observed in the presence of DAPI/calcofluor.

### Quantification of Swi6 fluorescence intensity at telomeres

To analyze the fluorescence intensity of Swi6 at telomeres in movies, we designed several regions of interests around Swi6 telomere foci and measured the total light content of these spots. An equivalent number of regions

of interest chosen in the nucleus in close proximity to the telomere spots were used as background and subtracted from telomere Swi6 signal. The signal was normalized to one at the beginning of mitosis. For the cell cycle analysis of Swi6 intensity (Fig. 5 D), multiple cells were quantified and the fluorescence intensity of Swi6 at telomeres was normalized to the intensity of the SPB signal in the same cell. Swi6 intensity was normalized to 1 in G2 cells [control: G2,  $n = 67$ ; anaphase,  $n = 53$ ; cytokinesis,  $n = 58$ ; Napp1: G2,  $n = 66$ ; anaphase,  $n = 88$ ].

#### Online supplemental material

Fig. S1 illustrates the reclustering of kinetochores at the end of mitosis during cytokinesis. Fig. S2 shows that Aurora B prevents telomere disjunction and nucleolar segregation. A condensin phosphomimetic mutant rescues this nucleolar segregation defect. Fig. S3 reveals that telomere nondisjunction leads to spindle collapse and cell death. Fig. S4 illustrates the presence of cells with stretched telomere signals in *rap1Δ* cells. The presence of these chromatin bridges with stretched telomeres slows down spindle elongation. The telomere dispersion defects in *rap1Δ* cells is *swi6*/HP1 dependent. Fig. S5 shows that Swi6 and Rad21 dissociates from telomeres at the metaphase-to-anaphase transition. Aurora prevents Rad21 dissociation from telomeres in a Swi6/HP1-dependent manner. Video 1 shows an example of fluorescent time-lapse imaging of telomeres, nucleolus, and spindle poles during mitosis. Table S1 shows strains used in this study. Online supplemental material is available at <http://www.jcb.org/cgi/content/full/jcb.201407016/DC1>.

We would like to thank J. Cooper, J.P. Javerzat, M. Yanagida, M. Flory, J. Kanoh, P. Bernard, and V. Geli for supplying strains; S. Hauf for supplying the *ark1-as3* mutant; Y. Watanabe for supplying the *cmd2* phosphorylation mutants; L.A. Rokeach for supplying the pREP-fib1-mRFP plasmid; and J.P. Javerzat and V. Geli for helpful discussions.

C. Serrurier was supported by a University Ministère de la Recherche et de la Technologie and Association pour la Recherche sur le Cancer fellowships. This work was funded by the ANR-blan120601 "Chromocatch" and l'Association de la Recherche sur le Cancer, fonctionnement, 2009. The microscopy equipment was funded by the Centre National de la Recherche Scientifique, l'ANR-blan120601, and l'Association de la Recherche sur le Cancer.

The authors declare no competing financial interests.

Submitted: 7 July 2014

Accepted: 9 February 2015

## References

- Adams, R.R., H. Maiato, W.C. Earnshaw, and M. Carmena. 2001. Essential roles of *Drosophila* inner centromere protein (INCENP) and aurora B in histone H3 phosphorylation, metaphase chromosome alignment, kinetochore disjunction, and chromosome segregation. *J. Cell Biol.* 153:865–880.
- Alfredsson-Timmings, J., F. Henningson, and P. Bjerling. 2007. The Ctr4 methyltransferase determines the subnuclear localization of the mating-type region in fission yeast. *J. Cell Sci.* 120:1935–1943. <http://dx.doi.org/10.1242/jcs.03457>
- Bähler, J., J.Q. Wu, M.S. Longtine, N.G. Shah, A. McKenzie III, A.B. Steever, A. Wach, P. Philippsen, and J.R. Pringle. 1998. Heterologous modules for efficient and versatile PCR-based gene targeting in *Schizosaccharomyces pombe*. *Yeast.* 14:943–951. [http://dx.doi.org/10.1002/\(SICI\)1097-0061\(199807\)14:10<943::AID-YEA292>3.0.CO;2-Y](http://dx.doi.org/10.1002/(SICI)1097-0061(199807)14:10<943::AID-YEA292>3.0.CO;2-Y)
- Beauregard, P.B., R. Guérin, C. Turcotte, S. Lindquist, and L.A. Rokeach. 2009. A nucleolar protein allows viability in the absence of the essential ER-residing molecular chaperone calnexin. *J. Cell Sci.* 122:1342–1351. <http://dx.doi.org/10.1242/jcs.040949>
- Bernard, P., J.F. Maure, J.F. Partridge, S. Genier, J.P. Javerzat, and R.C. Allshire. 2001. Requirement of heterochromatin for cohesion at centromeres. *Science.* 294:2539–2542. <http://dx.doi.org/10.1126/science.1064027>
- Carmena, M., M. Wheelock, H. Funabiki, and W.C. Earnshaw. 2012. The chromosomal passenger complex (CPC): from easy rider to the godfather of mitosis. *Nat. Rev. Mol. Cell Biol.* 13:789–803. <http://dx.doi.org/10.1038/nrm3474>
- Chang, Y.T., B.A. Moser, and T.M. Nakamura. 2013. Fission yeast shelterin regulates DNA polymerases and Rad3<sup>ATR</sup> kinase to limit telomere extension. *PLoS Genet.* 9:e1003936. <http://dx.doi.org/10.1371/journal.pgen.1003936>
- Chen, E.S., K. Zhang, E. Nicolas, H.P. Cam, M. Zofall, and S.I. Grewal. 2008. Cell cycle control of centromeric repeat transcription and heterochromatin assembly. *Nature.* 451:734–737. <http://dx.doi.org/10.1038/nature06561>
- Chikashige, Y., and Y. Hiraoka. 2001. Telomere binding of the Rap1 protein is required for meiosis in fission yeast. *Curr. Biol.* 11:1618–1623. [http://dx.doi.org/10.1016/S0960-9822\(01\)00457-2](http://dx.doi.org/10.1016/S0960-9822(01)00457-2)
- Cimini, D., X. Wan, C.B. Hirel, and E.D. Salmon. 2006. Aurora kinase promotes turnover of kinetochore microtubules to reduce chromosome segregation errors. *Curr. Biol.* 16:1711–1718. <http://dx.doi.org/10.1016/j.cub.2006.07.022>
- Clark, R.F., and S.C. Elgin. 1992. Heterochromatin protein 1, a known suppressor of position-effect variegation, is highly conserved in *Drosophila*. *Nucleic Acids Res.* 20:6067–6074. <http://dx.doi.org/10.1093/nar/20.22.6067>
- Cooper, J.P., E.R. Nimmo, R.C. Allshire, and T.R. Cech. 1997. Regulation of telomere length and function by a Myb-domain protein in fission yeast. *Nature.* 385:744–747. <http://dx.doi.org/10.1038/385744a0>
- Cooper, J.P., Y. Watanabe, and P. Nurse. 1998. Fission yeast Taz1 protein is required for meiotic telomere clustering and recombination. *Nature.* 392:828–831. <http://dx.doi.org/10.1038/33947>
- Corbett, K.D., C.K. Yip, L.S. Ee, T. Walz, A. Amon, and S.C. Harrison. 2010. The monopolin complex crosslinks kinetochore components to regulate chromosome-microtubule attachments. *Cell.* 142:556–567. <http://dx.doi.org/10.1016/j.cell.2010.07.017>
- Courtheoux, T., G. Gay, Y. Gachet, and S. Tournier. 2009. Ase1/Prc1-dependent spindle elongation corrects merotelically during anaphase in fission yeast. *J. Cell Biol.* 187:399–412. <http://dx.doi.org/10.1083/jcb.200902093>
- de Lange, T. 2009. How telomeres solve the end-protection problem. *Science.* 326:948–952. <http://dx.doi.org/10.1126/science.1170633>
- Dheur, S., S.J. Saupé, S. Genier, S. Vazquez, and J.P. Javerzat. 2011. Role for cohesin in the formation of a heterochromatic domain at fission yeast subtelomeres. *Mol. Cell Biol.* 31:1088–1097. <http://dx.doi.org/10.1128/MCB.01290-10>
- Ditchfield, C., V.L. Johnson, A. Tighe, R. Ellston, C. Haworth, T. Johnson, A. Mortlock, N. Keen, and S.S. Taylor. 2003. Aurora B couples chromosome alignment with anaphase by targeting BubR1, Mad2, and Cenp-E to kinetochores. *J. Cell Biol.* 161:267–280. <http://dx.doi.org/10.1083/jcb.200208091>
- Ekwall, K., J.P. Javerzat, A. Lorentz, H. Schmidt, G. Cranston, and R. Allshire. 1995. The chromodomain protein Swi6: a key component at fission yeast centromeres. *Science.* 269:1429–1431. <http://dx.doi.org/10.1126/science.7660126>
- Ekwall, K., E.R. Nimmo, J.P. Javerzat, B. Borgström, R. Egel, G. Cranston, and R. Allshire. 1996. Mutations in the fission yeast silencing factors *clr4<sup>+</sup>* and *rik1<sup>+</sup>* disrupt the localisation of the chromo domain protein Swi6p and impair centromere function. *J. Cell Sci.* 109:2637–2648.
- Ferreira, M.G., and J.P. Cooper. 2001. The fission yeast Taz1 protein protects chromosomes from Ku-dependent end-to-end fusions. *Mol. Cell.* 7:55–63. [http://dx.doi.org/10.1016/S1097-2765\(01\)00154-X](http://dx.doi.org/10.1016/S1097-2765(01)00154-X)
- Fischer, T., B. Cui, J. Dhakshnamoorthy, M. Zhou, C. Rubin, M. Zofall, T.D. Veenstra, and S.I. Grewal. 2009. Diverse roles of HP1 proteins in heterochromatin assembly and functions in fission yeast. *Proc. Natl. Acad. Sci. USA.* 106:8998–9003. <http://dx.doi.org/10.1073/pnas.0813063106>
- Fujita, I., Y. Nishihara, M. Tanaka, H. Tsujii, Y. Chikashige, Y. Watanabe, M. Saito, F. Ishikawa, Y. Hiraoka, and J. Kanoh. 2012. Telomere-nuclear envelope dissociation promoted by Rap1 phosphorylation ensures faithful chromosome segregation. *Curr. Biol.* 22:1932–1937. <http://dx.doi.org/10.1016/j.cub.2012.08.019>
- Funabiki, H., I. Hagan, S. Uzawa, and M. Yanagida. 1993. Cell cycle-dependent specific positioning and clustering of centromeres and telomeres in fission yeast. *J. Cell Biol.* 121:961–976. <http://dx.doi.org/10.1083/jcb.121.5.961>
- Gandhi, R., P.J. Gillespie, and T. Hirano. 2006. Human Wapl is a cohesin-binding protein that promotes sister-chromatid resolution in mitotic prophase. *Curr. Biol.* 16:2406–2417. <http://dx.doi.org/10.1016/j.cub.2006.10.061>
- Gay, G., T. Courtheoux, C. Reyes, S. Tournier, and Y. Gachet. 2012. A stochastic model of kinetochore-microtubule attachment accurately describes fission yeast chromosome segregation. *J. Cell Biol.* 196:757–774. <http://dx.doi.org/10.1083/jcb.201107124>
- Giet, R., and D.M. Glover. 2001. *Drosophila* Aurora B kinase is required for histone H3 phosphorylation and condensin recruitment during chromosome condensation and to organize the central spindle during cytokinesis. *J. Cell Biol.* 152:669–682. <http://dx.doi.org/10.1083/jcb.152.4.669>
- Giménez-Abián, J.F., I. Sumara, T. Hirota, S. Hauf, D. Gerlich, C. de la Torre, J. Ellenberg, and J.M. Peters. 2004. Regulation of sister chromatid cohesion between chromosome arms. *Curr. Biol.* 14:1187–1193. <http://dx.doi.org/10.1016/j.cub.2004.06.052>
- Gisselsson, D., and M. Höglund. 2005. Connecting mitotic instability and chromosome aberrations in cancer—can telomeres bridge the gap? *Semin. Cancer Biol.* 15:13–23. <http://dx.doi.org/10.1016/j.semcancer.2004.09.002>
- Gotta, M., and S.M. Gasser. 1996. Nuclear organization and transcriptional silencing in yeast. *Experientia.* 52:1136–1147. <http://dx.doi.org/10.1007/BF01952113>
- Gregan, J., C.G. Riedel, A.L. Pidoux, Y. Katou, C. Rumpf, A. Schleiffer, S.E. Kearsley, K. Shirahige, R.C. Allshire, and K. Nasmyth. 2007. The

- kinetochore proteins Pcs1 and Mde4 and heterochromatin are required to prevent merotelic orientation. *Curr. Biol.* 17:1190–1200. <http://dx.doi.org/10.1016/j.cub.2007.06.044>
- Gregan, J., S. Polakova, L. Zhang, I.M. Tolić-Nørrelykke, and D. Cimini. 2011. Merotelic kinetochore attachment: causes and effects. *Trends Cell Biol.* 21:374–381. <http://dx.doi.org/10.1016/j.tcb.2011.01.003>
- Hall, I.M., K. Noma, and S.I. Grewal. 2003. RNA interference machinery regulates chromosome dynamics during mitosis and meiosis in fission yeast. *Proc. Natl. Acad. Sci. USA.* 100:193–198. <http://dx.doi.org/10.1073/pnas.232688099>
- Harland, J.L., Y.T. Chang, B.A. Moser, and T.M. Nakamura. 2014. Tpz1-Ccq1 and Tpz1-Poz1 interactions within fission yeast shelterin modulate Ccq1 Thr93 phosphorylation and telomerase recruitment. *PLoS Genet.* 10:e1004708. <http://dx.doi.org/10.1371/journal.pgen.1004708>
- Hauf, S., A. Biswas, M. Langeegger, S.A. Kawashima, T. Tsukahara, and Y. Watanabe. 2007. Aurora controls sister kinetochore mono-orientation and homolog bi-orientation in meiosis-I. *EMBO J.* 26:4475–4486. <http://dx.doi.org/10.1038/sj.emboj.7601880>
- Hediger, F., F.R. Neumann, G. Van Houwe, K. Dubrana, and S.M. Gasser. 2002. Live imaging of telomeres: yKu and Sir proteins define redundant telomere-anchoring pathways in yeast. *Curr. Biol.* 12:2076–2089. [http://dx.doi.org/10.1016/S0960-9822\(02\)01338-6](http://dx.doi.org/10.1016/S0960-9822(02)01338-6)
- Hentges, P., B. Van Driessche, L. Tafforeau, J. Vandenhoute, and A.M. Carr. 2005. Three novel antibiotic marker cassettes for gene disruption and marker switching in *Schizosaccharomyces pombe*. *Yeast.* 22:1013–1019. <http://dx.doi.org/10.1002/yea.1291>
- Hirano, T., S. Funahashi, T. Uemura, and M. Yanagida. 1986. Isolation and characterization of *Schizosaccharomyces pombe* cutmutants that block nuclear division but not cytokinesis. *EMBO J.* 5:2973–2979.
- James, T.C., J.C. Eissenberg, C. Craig, V. Dietrich, A. Hobson, and S.C. Elgin. 1989. Distribution patterns of HP1, a heterochromatin-associated nonhistone chromosomal protein of *Drosophila*. *Eur. J. Cell Biol.* 50:170–180.
- Kanoh, J., and F. Ishikawa. 2001. spRap1 and spRif1, recruited to telomeres by Taz1, are essential for telomere function in fission yeast. *Curr. Biol.* 11:1624–1630. [http://dx.doi.org/10.1016/S0960-9822\(01\)00503-6](http://dx.doi.org/10.1016/S0960-9822(01)00503-6)
- Kanoh, J., M. Sadaie, T. Urano, and F. Ishikawa. 2005. Telomere binding protein Taz1 establishes Swi6 heterochromatin independently of RNAi at telomeres. *Curr. Biol.* 15:1808–1819. <http://dx.doi.org/10.1016/j.cub.2005.09.041>
- Knowlton, A.L., W. Lan, and P.T. Stukenberg. 2006. Aurora B is enriched at merotelic attachment sites, where it regulates MCAK. *Curr. Biol.* 16:1705–1710. <http://dx.doi.org/10.1016/j.cub.2006.07.057>
- Koch, A., K. Krug, S. Pengelley, B. Macek, and S. Hauf. 2011. Mitotic substrates of the kinase aurora with roles in chromatin regulation identified through quantitative phosphoproteomics of fission yeast. *Sci. Signal.* 4:rs6.
- Kotwaliwale, C.V., S.B. Frei, B.M. Stern, and S. Biggins. 2007. A pathway containing the Ipl1/aurora protein kinase and the spindle midzone protein Ase1 regulates yeast spindle assembly. *Dev. Cell.* 13:433–445. <http://dx.doi.org/10.1016/j.devcel.2007.07.003>
- Kueng, S., B. Hegemann, B.H. Peters, J.J. Lipp, A. Schleiffer, K. Mechtler, and J.M. Peters. 2006. Wapl controls the dynamic association of cohesin with chromatin. *Cell.* 127:955–967. <http://dx.doi.org/10.1016/j.cell.2006.09.040>
- Leversson, J.D., H.K. Huang, S.L. Forsburg, and T. Hunter. 2002. The *Schizosaccharomyces pombe* aurora-related kinase Ark1 interacts with the inner centromere protein Pic1 and mediates chromosome segregation and cytokinesis. *Mol. Biol. Cell.* 13:1132–1143. <http://dx.doi.org/10.1091/mbc.01-07-0330>
- Lipp, J.J., T. Hirota, I. Poser, and J.M. Peters. 2007. Aurora B controls the association of condensin I but not condensin II with mitotic chromosomes. *J. Cell Sci.* 120:1245–1255. <http://dx.doi.org/10.1242/jcs.03425>
- Losada, A., M. Hirano, and T. Hirano. 2002. Cohesin release is required for sister chromatid resolution, but not for condensin-mediated compaction, at the onset of mitosis. *Genes Dev.* 16:3004–3016. <http://dx.doi.org/10.1101/gad.249202>
- Maillet, L., C. Boscheron, M. Gotta, S. Marcand, E. Gilson, and S.M. Gasser. 1996. Evidence for silencing compartments within the yeast nucleus: a role for telomere proximity and Sir protein concentration in silencer-mediated repression. *Genes Dev.* 10:1796–1811. <http://dx.doi.org/10.1101/gad.10.14.1796>
- Miller, K.M., M.G. Ferreira, and J.P. Cooper. 2005. Taz1, Rap1 and Rif1 act both interdependently and independently to maintain telomeres. *EMBO J.* 24:3128–3135. <http://dx.doi.org/10.1038/sj.emboj.7600779>
- Misteli, T., and E. Soutoglou. 2009. The emerging role of nuclear architecture in DNA repair and genome maintenance. *Nat. Rev. Mol. Cell Biol.* 10:243–254. <http://dx.doi.org/10.1038/nrm2651>
- Miyoshi, T., J. Kanoh, M. Saito, and F. Ishikawa. 2008. Fission yeast Pot1-Tpp1 protects telomeres and regulates telomere length. *Science.* 320:1341–1344. <http://dx.doi.org/10.1126/science.1154819>
- Mora-Bermúdez, F., D. Gerlich, and J. Ellenberg. 2007. Maximal chromosome compaction occurs by axial shortening in anaphase and depends on Aurora kinase. *Nat. Cell Biol.* 9:822–831. <http://dx.doi.org/10.1038/ncb1606>
- Moreno, S., A. Klar, and P. Nurse. 1991. Molecular genetic analysis of fission yeast *Schizosaccharomyces pombe*. *Methods Enzymol.* 194:795–823. [http://dx.doi.org/10.1016/0076-6879\(91\)94059-L](http://dx.doi.org/10.1016/0076-6879(91)94059-L)
- Morishita, J., T. Matsusaka, G. Goshima, T. Nakamura, H. Tatebe, and M. Yanagida. 2001. Bir1/Cut17 moving from chromosome to spindle upon the loss of cohesion is required for condensation, spindle elongation and repair. *Genes Cells.* 6:743–763. <http://dx.doi.org/10.1046/j.1365-2443.2001.00459.x>
- Moser, B.A., Y.T. Chang, J. Kosti, and T.M. Nakamura. 2011. Tel1<sup>ATM</sup> and Rad3<sup>ATR</sup> kinases promote Ccq1-Est1 interaction to maintain telomeres in fission yeast. *Nat. Struct. Mol. Biol.* 18:1408–1413. <http://dx.doi.org/10.1038/nsmb.2187>
- Motwani, T., R. Doris, S.G. Holmes, and M.R. Flory. 2010. Ccq1p and the condensin proteins Cut3p and Cut14p prevent telomere entanglements in the fission yeast *Schizosaccharomyces pombe*. *Eukaryot. Cell.* 9:1612–1621. <http://dx.doi.org/10.1128/EC.00339-09>
- Nakayama, J., J.C. Rice, B.D. Strahl, C.D. Allis, and S.I. Grewal. 2001. Role of histone H3 lysine 9 methylation in epigenetic control of heterochromatin assembly. *Science.* 292:110–113. <http://dx.doi.org/10.1126/science.1060118>
- Nakazawa, N., T. Nakamura, A. Kokubu, M. Ebe, K. Nagao, and M. Yanagida. 2008. Dissection of the essential steps for condensin accumulation at kinetochores and rDNAs during fission yeast mitosis. *J. Cell Biol.* 180:1115–1131. <http://dx.doi.org/10.1083/jcb.200708170>
- Nakazawa, N., R. Mehrotra, M. Ebe, and M. Yanagida. 2011. Condensin phosphorylated by the Aurora-B-like kinase Ark1 is continuously required until telophase in a mode distinct from Top2. *J. Cell Sci.* 124:1795–1807. <http://dx.doi.org/10.1242/jcs.078733>
- Nandakumar, J., and T.R. Cech. 2013. Finding the end: recruitment of telomerase to telomeres. *Nat. Rev. Mol. Cell Biol.* 14:69–82. <http://dx.doi.org/10.1038/nrm3505>
- Neurohr, G., A. Naegeli, I. Titos, D. Theler, B. Greber, J. Díez, T. Gabaldón, M. Mendoza, and Y. Barral. 2011. A midzone-based ruler adjusts chromosome compaction to anaphase spindle length. *Science.* 332:465–468. <http://dx.doi.org/10.1126/science.1201578>
- Nonaka, N., T. Kitajima, S. Yokobayashi, G. Xiao, M. Yamamoto, S.I. Grewal, and Y. Watanabe. 2002. Recruitment of cohesin to heterochromatic regions by Swi6/HP1 in fission yeast. *Nat. Cell Biol.* 4:89–93. <http://dx.doi.org/10.1038/ncb739>
- Nozawa, R.S., K. Nagao, H.T. Masuda, O. Iwasaki, T. Hirota, N. Nozaki, H. Kimura, and C. Obuse. 2010. Human POGZ modulates dissociation of HP1 $\alpha$  from mitotic chromosome arms through Aurora B activation. *Nat. Cell Biol.* 12:719–727. <http://dx.doi.org/10.1038/ncb2075>
- Ono, T., Y. Fang, D.L. Spector, and T. Hirano. 2004. Spatial and temporal regulation of Condensins I and II in mitotic chromosome assembly in human cells. *Mol. Biol. Cell.* 15:3296–3308. <http://dx.doi.org/10.1091/mbc.E04-03-0242>
- Palladino, F., T. Laroche, E. Gilson, A. Axelrod, L. Pillus, and S.M. Gasser. 1993. SIR3 and SIR4 proteins are required for the positioning and integrity of yeast telomeres. *Cell.* 75:543–555. [http://dx.doi.org/10.1016/0092-8674\(93\)90388-7](http://dx.doi.org/10.1016/0092-8674(93)90388-7)
- Pardo, M., and P. Nurse. 2005. The nuclear rim protein Amo1 is required for proper microtubule cytoskeleton organisation in fission yeast. *J. Cell Sci.* 118:1705–1714. <http://dx.doi.org/10.1242/jcs.02305>
- Petersen, J., J. Paris, M. Willer, M. Philippe, and I.M. Hagan. 2001. The *S. pombe* aurora-related kinase Ark1 associates with mitotic structures in a stage dependent manner and is required for chromosome segregation. *J. Cell Sci.* 114:4371–4384.
- Pinsky, B.A., C. Kung, K.M. Shokat, and S. Biggins. 2006. The Ipl1-Aurora protein kinase activates the spindle checkpoint by creating unattached kinetochores. *Nat. Cell Biol.* 8:78–83. <http://dx.doi.org/10.1038/ncb1341>
- Poon, B.P., and K. Mekhail. 2011. Cohesin and related coiled-coil domain-containing complexes physically and functionally connect the dots across the genome. *Cell Cycle.* 10:2669–2682. <http://dx.doi.org/10.4161/cc.10.16.17113>
- Rumpf, C., L. Cipak, A. Schleiffer, A. Pidoux, K. Mechtler, I.M. Tolić-Nørrelykke, and J. Gregan. 2010. Laser microscopy provides evidence for merotelic kinetochore attachments in fission yeast cells lacking Pcs1 or Clr4. *Cell Cycle.* 9:3997–4004. <http://dx.doi.org/10.4161/cc.9.19.13233>
- Sakuno, T., K. Tada, and Y. Watanabe. 2009. Kinetochore geometry defined by cohesion within the centromere. *Nature.* 458:852–858. <http://dx.doi.org/10.1038/nature07876>
- Sampath, S.C., R. Ohi, O. Leismann, A. Salic, A. Pozniakovski, and H. Funabiki. 2004. The chromosomal passenger complex is required for chromatin-induced microtubule stabilization and spindle assembly. *Cell.* 118:187–202. <http://dx.doi.org/10.1016/j.cell.2004.06.026>



- Sexton, T., H. Schober, P. Fraser, and S.M. Gasser. 2007. Gene regulation through nuclear organization. *Nat. Struct. Mol. Biol.* 14:1049–1055. <http://dx.doi.org/10.1038/nsmb1324>
- Shintomi, K., and T. Hirano. 2009. Releasing cohesin from chromosome arms in early mitosis: opposing actions of Wapl-Pds5 and Sgo1. *Genes Dev.* 23:2224–2236. <http://dx.doi.org/10.1101/gad.1844309>
- Steigemann, P., C. Wurzenberger, M.H. Schmitz, M. Held, J. Guizetti, S. Maar, and D.W. Gerlich. 2009. Aurora B-mediated abscission checkpoint protects against tetraploidization. *Cell.* 136:473–484. <http://dx.doi.org/10.1016/j.cell.2008.12.020>
- Sugiyama, T., H.P. Cam, R. Sugiyama, K. Noma, M. Zofall, R. Kobayashi, and S.I. Grewal. 2007. SHREC, an effector complex for heterochromatic transcriptional silencing. *Cell.* 128:491–504. <http://dx.doi.org/10.1016/j.cell.2006.12.035>
- Sumara, I., E. Vorlaufer, P.T. Stukenberg, O. Kelm, N. Redemann, E.A. Nigg, and J.M. Peters. 2002. The dissociation of cohesin from chromosomes in prophase is regulated by Polo-like kinase. *Mol. Cell.* 9:515–525. [http://dx.doi.org/10.1016/S1097-2765\(02\)00473-2](http://dx.doi.org/10.1016/S1097-2765(02)00473-2)
- Sutani, T., T. Yuasa, T. Tomonaga, N. Dohmae, K. Takio, and M. Yanagida. 1999. Fission yeast condensin complex: essential roles of non-SMC subunits for condensation and Cdc2 phosphorylation of Cut3/SMC4. *Genes Dev.* 13:2271–2283. <http://dx.doi.org/10.1101/gad.13.17.2271>
- Tada, K., H. Susumu, T. Sakuno, and Y. Watanabe. 2011. Condensin association with histone H2A shapes mitotic chromosomes. *Nature.* 474:477–483. <http://dx.doi.org/10.1038/nature10179>
- Tanaka, T.U., N. Rachidi, C. Janke, G. Pereira, M. Galova, E. Schiebel, M.J. Stark, and K. Nasmyth. 2002. Evidence that the Ipl1-Sli15 (Aurora kinase-INCENP) complex promotes chromosome bi-orientation by altering kinetochore-spindle pole connections. *Cell.* 108:317–329. [http://dx.doi.org/10.1016/S0092-8674\(02\)00633-5](http://dx.doi.org/10.1016/S0092-8674(02)00633-5)
- Thuriaux, P., M. Sipiczki, and P.A. Fantes. 1980. Genetical analysis of a sterile mutant by protoplast fusion in the fission yeast *Schizosaccharomyces pombe*. *J. Gen. Microbiol.* 116:525–528.
- Titos, I., T. Ivanova, and M. Mendoza. 2014. Chromosome length and perinuclear attachment constrain resolution of DNA intertwinings. *J. Cell Biol.* 206:719–733. <http://dx.doi.org/10.1083/jcb.201404039>
- Tomita, K., and J.P. Cooper. 2008. Fission yeast Ccq1 is telomerase recruiter and local checkpoint controller. *Genes Dev.* 22:3461–3474. <http://dx.doi.org/10.1101/gad.498608>
- Tóth, A., K.P. Rabitsch, M. Gálová, A. Schleiffer, S.B. Buonomo, and K. Nasmyth. 2000. Functional genomics identifies monopolin: a kinetochore protein required for segregation of homologs during meiosis I. *Cell.* 103:1155–1168. [http://dx.doi.org/10.1016/S0092-8674\(00\)00217-8](http://dx.doi.org/10.1016/S0092-8674(00)00217-8)
- Tournier, S., Y. Gachet, V. Buck, J.S. Hyams, and J.B. Millar. 2004. Disruption of astral microtubule contact with the cell cortex activates a Bub1, Bub3, and Mad3-dependent checkpoint in fission yeast. *Mol. Biol. Cell.* 15:3345–3356. <http://dx.doi.org/10.1091/mbc.E04-03-0256>
- Uhlmann, F., F. Lottspeich, and K. Nasmyth. 1999. Sister-chromatid separation at anaphase onset is promoted by cleavage of the cohesin subunit Scc1. *Nature.* 400:37–42. <http://dx.doi.org/10.1038/21831>
- Uzawa, S., and M. Yanagida. 1992. Visualization of centromeric and nucleolar DNA in fission yeast by fluorescence in situ hybridization. *J. Cell Sci.* 101:267–275.
- Vanoosthuyse, V., S. Prykhozhij, and K.G. Hardwick. 2007. Shugoshin 2 regulates localization of the chromosomal passenger proteins in fission yeast mitosis. *Mol. Biol. Cell.* 18:1657–1669. <http://dx.doi.org/10.1091/mbc.E06-10-0890>
- Vassetzky, N.S., F. Gaden, C. Brun, S.M. Gasser, and E. Gilson. 1999. Taz1p and Teb1p, two telobox proteins in *Schizosaccharomyces pombe*, recognize different telomere-related DNA sequences. *Nucleic Acids Res.* 27:4687–4694. <http://dx.doi.org/10.1093/nar/27.24.4687>
- Waizenegger, I.C., S. Hauf, A. Meinke, and J.M. Peters. 2000. Two distinct pathways remove mammalian cohesin from chromosome arms in prophase and from centromeres in anaphase. *Cell.* 103:399–410. [http://dx.doi.org/10.1016/S0092-8674\(00\)00132-X](http://dx.doi.org/10.1016/S0092-8674(00)00132-X)
- Yamagishi, Y., T. Honda, Y. Tanno, and Y. Watanabe. 2010. Two histone marks establish the inner centromere and chromosome bi-orientation. *Science.* 330:239–243. <http://dx.doi.org/10.1126/science.1194498>
- Yamazaki, H., Y. Tarumoto, and F. Ishikawa. 2012. Tel1<sup>ATM</sup> and Rad3<sup>ATR</sup> phosphorylate the telomere protein Ccq1 to recruit telomerase and elongate telomeres in fission yeast. *Genes Dev.* 26:241–246. <http://dx.doi.org/10.1101/gad.177873.111>